

**A THESIS
FOR THE DEGREE OF MASTER OF SCIENCE**

**Antioxidant and Anti-inflammatory
Effects of Active Compounds Isolated
from *Ecklonia cava***

Sung-Myung Kang

Department of Aquatic Life Medicine

**GRADUATE SCHOOL
CHEJU NATIONAL UNIVERSITY**

2009. 02.

**Antioxidant and Anti-inflammatory Effects of
Active Compounds Isolated from *Ecklonia cava*.**

Sung-Myung Kang

(Supervised by Professor You-Jin Jeon)

**A thesis submitted in partial fulfillment of the requirement for the degree of
Master of Science
2009. 02.**

This thesis has been examined and approved by`

Lee Ki Wan

Thesis director, Ki-Wan Lee, Professor of Marine Life Science

[Signature]

Moon-Soo Heo, Professor of Aquatic Life Medicine

[Signature]

You-Jin Jeon, Professor of Aquatic Life Medicine

Date

**Department of Aquatic Life Medicine
GRADUATE SCHOOL
CHEJU NATIONAL UNIVERSITY**

CONTENTS

국문초록.....	iv
LIST OF FIGURES.....	viii
LIST OF TABLES.....	xiii
Part I. Antioxidant polyphenol compounds isolated from <i>E. cava</i>	1
ABSTRACT	2
INTRODUCTION	3
MATERIALS & METHODS	
Chemicals.....	5
Plant material.....	5
Extraction and isolation.....	7
DPPH radical scavenging assay using an ESR spectrometer.....	9
Alkyl radical scavenging assay using an ESR spectrometer.....	9
Hydroxyl radical scavenging assay using an ESR spectrometer.....	10
Superoxide radical scavenging using an ESR spectrometer.....	10
Antioxidant activities by Vero cell lines	
Cell culture.....	11
Intracellular reactive oxygen species (ROS) measurement.....	11
Assessment of cell cytotoxicity.....	12
Comet assay.....	12
Statistical analysis.....	13
RESULTS	
Isolation and purification of active compounds.....	14
DPPH radical scavenging assay.....	35

Alkyl radical scavenging assay.....	37
Hydroxyl radical scavenging assay.....	39
Superoxide radical scavenging assay.....	41
Intracellular reactive oxygen species (ROS) measurement	43
Protective effect against H ₂ O ₂ -induced cell damage.....	44
DISCUSSION.....	50
Part II. Anti-inflammatory activity of polysaccharide purified from	
 AMG extract of <i>E. cava</i> in LPS-stimulated RAW 264.7 macrophages	
ABSTRACT.....	53
INTRODUCTION.....	54
MATERIALS & METHODS	
Plant material and extraction.....	56
Molecular weight fractionation of AMG extract.....	56
Crude polysaccharide separation.....	57
Anion-exchange chromatography.....	57
Gel filtration chromatography.....	57
Determination of the Molecular Mass of purified polysaccharide.....	58
Neutral sugar composition.....	58
Sulfate content analysis.....	58
Cell culture.....	59
Nitrite assay.....	59
Western bolt analysis of COX-2 and iNOS in RAW 264.7 cells.....	59
PGE ₂ enzyme-linked immunosorbent assay (ELISA).....	60

RESULTS

Isolation and purification of active compounds isolated from <i>Ecklonia cava</i> for anti-inflammation in RAW264.7 cell.....	61
Monosugar composition and sulfate contents assays.....	64
Determination of Molecular Mass purified polysaccharide.....	66
Inhibition of NO (nitric oxide) production by separated polysaccharide fraction.....	67
Inhibition of iNOS expression and NO production by isolated PPA.....	70
Inhibition of PPA on COX-2 protein expression in RAW 264.7 cells.....	72
Inhibition of PPA on PGE ₂ production in RAW264.7 cells.....	73
DISCUSSION	75
REFERENCE	77
ACKNOWLEDGEMENT	84

국문 초록

이 연구는 감태로부터 생리활성 성분을 분리·정제한 후 항산화와 항염증 활성을 측정하여 Part I 과 Part II 로 분리하여 그 내용과 결과를 요약하였다.

PART I. 감태 유래 폴리페놀 화합물의 항산화 활성

활성 산소종(ROS, reactive oxygen species)이란 최외각 전자 궤도에 쌍을 이루지 못하는 전자를 가지는 자유 라디칼 (free radical)과 여기에서 파생된 여러 가지 산소화합물의 집합이라 할 수 있다. ROS는 인간을 비롯한 동식물의 체내에 세균과 바이러스 및 곰팡이 등의 이물질이 침입하면 이것들을 공격하여 제거하는 생체 방어 역할을 하고 있다. 그러나 ROS는 반응성이 매우 강하고 불안정하여 세포 구성 성분들인 지질과 단백질 및 당 그리고 DNA 등에 대하여 비선택적이고 비가역적인 파괴작용을 하게 된다. 이러한 결과로 노화 및 암을 비롯하여 뇌질환과 심장 질환 및 동맥 경화 그리고 피부 와 소화기 질환과 염증 또는 자가면역질환과 같은 각종 질병을 일으키는 것으로 알려져 있다. 지금까지 알려진 항산화제가 약한 활성과 독성 및 사용상의 한계로 인한 많은 문제점을 내포하기 때문에 천연물에서 항산화제의 개발이 요구되고 있는 실정이다. 일반적으로 천연물의 여러 가지 성분들은 conjugated double bond와 polyphenol 구조 및 SH 기를 갖는 화합물 그리고 alkaloids와 유기산 등이 항산화 활성을 갖는 것으로 보고되어 있다.

감태(*Ecklonia cava*)는 갈조식물 다시마목 (Laminariales) 미역과 (Alariaceae)에 속하며 주로 우리나라 동·남해안과 제주 연안 및 일본에 서식하고 있다. 이들은 전복과 소라의 먹이가 되며 예전에는 주요 알긴산 제조 원료로 사용되었으나 최근에는 풍조 (drifted algae)로 유기 활성 물질 연구 대상종으로 부각되었다. 감태의 밝

혀진 주요 생리활성 물질은 phlorotannin 계열과 polysaccharide 계열이 있으며 HIV-1 역전사 효소 저해활성과 Xanthin oxidase 저해활성 및 tryosinase 활성억제효과 그리고 항응고 활성 및 항암 활성 등이 연구 보고된 바 있다.

Part 1에서는 감태 생리활성 성분을 80% methanol을 이용하여 추출하여 ethyl acetate을 첨가하여 분획하였고, 이렇게 분획된 ethyl acetate fraction은 celite column chromatography에 충전 후 hexane과 dichloro-methane 및 diethyl ether 그리고 methanol fraction으로 분획하여 fraction 별 항산화 실험을 측정한 결과, diethyl ether fraction에서 가장 높게 항산화 활성을 보였다. Diethyl ether fraction은 Silica column 와 Sephadex LH-20 column chromatography를 통해 정제된 후 RP-HPLC를 이용하여 분석하였고 분리된 4개의 성분을 LC-mass 와 NMR을 통하여 구조 분석 하였다. 구조 분석 결과 4개의 성분에서 3개의 신물질과 이미 알려진 1개의 물질임을 확인 할 수 있었다. 구조가 밝혀진 4개 성분에 대한 항산화 활성은 ESR을 이용하여 라디칼 소거활성이 측정되었고, 정상세포인 Vero cell의 산화적 손상 억제 활성을 측정하였다. 그 결과 4개의 성분들은 모두 높은 라디칼 소거 활성을 나타냈으며 Vero cell에 대한 산화적 손상이 억제 되어 우수한 세포 보호효과를 나타냈다.

PART II. 감태 유래 다당류의 항염증 활성

염증은 손상에 대한 살아 있는 조직의 반응으로 생체 조직이 물리적이거나 기계적으로 또는 화학적이거나 생물학적 자극에 의하여 손상을 받았을 때 이를 국소화 시키고 정상 부위로 되돌리려는 생체 방어기전이다. 이는 생체에 유해한 자극이 가해지고 난 후의 방어기전으로부터 수복 과정까지의 모든 경과를 가리킨다. 이러한 염증 반응은 혈관이 있는 조직에서만 일어날 수 있는 특징을 가지고 있다. 제 1기는 혈관의 확장과 혈관 투과성의 항진, 제2기는 백혈구의 유주와 점착, 그리고 제3기

는 육아조직의 형성과 혈관신생을 보여준다. 염증 진행은 염증부위로부터 히스타민과 브라디키닌 및 프로스타글라딘 등의 화학물질이 분비되어 진행된다. 국소증상은 발적이나 종창과 열감이나 동통 및 부종 또는 기증장애 등의 징후가 있다. 면역 반응이나 백혈구 증가 같은 전신증상을 나타내는 경우가 있다. 특히 염증 부위의 활성화된 macrophage는 cytokine과 prostaglandin 및 nitric oxide 등을 생성함으로써 염증 매개 역할을 한다.

NO(nitric oxide)는 라디칼을 가진 가스성의 물질이며, 생체 내에서 짧은 시간 동안만 존재한다. NO는 생체 내에서 심혈관계의 항상성 조절과 혈액 응고 및 신경 전달 등에서 중요한 역할을 하지만 독성을 나타내기도 한다. NO의 과잉 생성은 여러 징후들(circulatory shock, atherosclerosis, cardiac allograft rejection, chronic inflammation, cardiac infarction, cancer)과 연관 있음이 밝혀지고 있다. NO는 L-arginine에서 촉매제인 nitric oxide synthase (NOS)의 영향으로 L-citrulline으로 바뀌며, 이 때 NO가 생성된다. NOS의 isoform은 크게 3가지이며 (nNOS (neuronal), eNOS (endothelial), iNOS (inducible)) nNOS와 eNOS는 constitutive 하지만 inducible form은 iNOS 뿐이다. iNOS는 LPS와 cytokine의 자극인자에 의해서 macrophage와 같은 염증세포에서 유도되어 constitutive form 보다 1000배나 많은 NO를 생성하게 된다. 이때 생성된 다량의 NO는 염증 반응을 야기하거나 cyclooxygenase (COX) 의 활성을 촉진시키게되어 염증 반응을 심화시킨다. NO 생성 억제제는 항염증제 기전을 연구하는데 있어 좋은 치료 target 이라고 할 수 있다.

이 Part 2 에서 수용성 활성 물질 제조는 효소적 추출 방법을 이용하여 건조된 감태로부터 당 분해효소와 단백질 분해효소로 추출하였다. 각 효소 별 추출물에 대한 항염증 측정 결과는 AMG 추출물이 높은 활성과 추출 수율을 가지고 있어 AMG 효소 추출물로 항염증 물질을 분리·정제 하였다. AMG 효소추출물을 50kDa molecular weight membrane으로 분획하였고 50kDa 이상 분획물과 50kDa 이하

분획물의 염증 활성을 측정한 결과는 50kDa 이상 분획물에서 더 높은 활성을 보였으며 50kDa 이상 분획물을 에탄올 침전법을 이용하여 polysaccharide를 침전시켜 분리하였다. 이 두 개의 분획물을 가지고 항염증 실험을 한 결과는 침전된 분획물 (Polysaccharide fraction)이 높은 염증 억제 활성을 나타내어 이를 정제 하였다. 침전된 polysaccharide 분획물은 DEAE-cellulose와 Sepharose-4B 컬럼을 이용하여 정제되었고 Bio-LC로 당 성분이 분석 되었다. 이 분석 결과는 Fucose 함량이 82%였으며 Galactose 함량은 11% 이었다. 또한 황산기 함량을 측정한 결과 정제된 polysaccharide는 0.92%의 황산기를 함유하고 있었으며 이를 통하여 정제된 polysaccharide는 해조 유래 다당류인 sulfated-fucoidan이라 보여진다. Polysaccharide를 이용한 항염증 실험한 결과는 NO와 PGE₂ 생성 및 iNOS 그리고 COX-2 발현을 농도 의존적으로 억제 하였다.

이러한 결과를 종합하면 감태의 생리 활성 성분은 항산화 활성 및 항염증 활성에 효과적임이 입증하였고, 기존의 합성 항산화제 및 항염증제가 가지는 인체 안전성 문제를 해결하는 효시적 연구이다.

LIST OF FIGURE

- Fig. 1-1. The photograph of a brown alga, *Ecklonia cava*.
- Fig. 1-2. Isolation and purification scheme of the active compounds from *E. cava*.
- Fig. 1-3. DPPH radical scavenging activities of fractions separated by sephadex LH-20 chromatography from diethyl ether fraction. Experiments were performed in triplicate and the data are expressed as mean \pm SE.
- Fig. 1-4. Chemical structure of the 6,6'-bieckol (BEK) isolated *E.cava*.
- Fig. 1-5. The LC-mass spectrum of 6,6'-bieckol (BEK) isolated form *E. cava*.
- Fig. 1-6. Proton and Carbon NMR spectrum of 6,6'-bieckol (BEK).
- Fig. 1-7. Chemical structure of the pyrogallol-6,6'-bieckol (PYB) isolated *E.cava*.
- Fig. 1-8. The LC-mass spectrum of pyrogallol-6,6'-bieckol (PYB) isolated form *E. cava*.
- Fig. 1-9. Proton and Carbon NMR spectrum of pyrogallol-6,6'-bieckol (PYB).
- Fig. 1-10. Chemical structure of the 2,7''-phloroglucinol-6,6'-bieckol (PHB) isolated *E.cava*.
- Fig. 1-11. The LC mass spectrum of 2,7''-phloroglucinol-6,6'-bieckol (PHB) isolated form *E. cava*
- Fig. 1-12. Proton and Carbon NMR spectrum of 2,7''-phloroglucinol-6,6'-bieckol (PHB).
- Fig. 1-13. Chemical structure of the phloroglucinol-pyrogallol-6,6'-bieckol (PPB) isolated *E.cava*.
- Fig. 1-14. The LC mass spectrum of the phloroglucinol-pyrogallol-6,6'-bieckol (PPB) isolated form *E. cava*
- Fig. 1-15. Proton and Carbon NMR spectrum of phloroglucinol-pyrogallol-6,6'-

bieckol (PPB).

Fig. 1-16. DPPH radical scavenging activity of the active compounds isolated from *E. cava*. Experiments were performed in triplicate and the data are expressed as mean \pm SE.

Fig. 1-17. Alkyl radical scavenging activity of the active compounds isolated from *E. cava*. Experiments were performed in triplicate and the data are expressed as mean \pm SE.

Fig. 1-18. Hydroxyl radical scavenging activity of the active compounds isolated from *E. cava*. Experiments were performed in triplicate and the data are expressed as mean \pm SE.

Fig. 1-19. Superoxide radical scavenging activity of the active compounds isolated from *E. cava*. Experiments were performed in triplicate and the data are expressed as mean \pm SE.

Fig. 1-20. Effect of the compounds isolated from *E. cava* on scavenging reactive oxygen species. The intracellular reactive oxygen species generated was detected by DCFH-DA method. Experiments were performed in triplicate and the data are expressed as mean \pm SE.

Fig. 1-21. Photomicrographs of DNA damage and migration observed under PYB isolated *E. cava*. A, control; B, 100uM H₂O₂; C, 25 ug/ml of compound + 100uM H₂O₂; D, 50 ug/ml of compound + 100uM H₂O₂.

Fig. 1-22. Inhibitory effect of different concentrations of PYB isolated *E. cava* on H₂O₂ induced DNA damage. The damage cells on H₂O₂-treatment were determined by comet assay. □, % Fluorescence in tail; ◆, Inhibitory effect of cell damage. Experiments were performed in triplicate and the data are

expressed as mean \pm SE.

Fig. 1-23. Photomicrographs of DNA damage and migration observed under BEK isolated *E. cava*. A, control; B, 100 μ M H₂O₂ ; C, 25 μ g/ml of compound + 100 μ M H₂O₂ ; D, 50 μ g/ml of compound + 100 μ M H₂O₂.

Fig. 1-24. Inhibitory effect of different concentrations of BEK isolated *E. cava* on H₂O₂ induced DNA damage. The damage cells on H₂O₂-treatment were determined by comet assay. \square , % Fluorescence in tail; \blacklozenge , Inhibitory effect of cell damage. Experiments were performed in triplicate and the data are expressed as mean \pm SE.

Fig. 1-25. Photomicrographs of DNA damage and migration observed under PHB isolated *E. cava*. A, control; B, 100 μ M H₂O₂ ; C, 25 μ g/ml of compound + 100 μ M H₂O₂ ; D, 50 μ g/ml of compound + 100 μ M H₂O₂.

Fig. 1-26. Inhibitory effect of different concentrations of PHB isolated *E. cava* on H₂O₂ induced DNA damage. The damage cells on H₂O₂-treatment were determined by comet assay. \square , % Fluorescence in tail; \blacklozenge , Inhibitory effect of cell damage. Experiments were performed in triplicate and the data are expressed as mean \pm SE.

Fig. 1-27. Photomicrographs of DNA damage and migration observed under PPB isolated *E. cava*. A, control; B, 100 μ M H₂O₂ ; C, 25 μ g/ml of compound + 100 μ M H₂O₂ ; D, 50 μ g/ml of compound + 100 μ M H₂O₂.

Fig. 1-28. Inhibitory effect of different concentrations of PPB isolated *E. cava* on H₂O₂ induced DNA damage. The damage cells on H₂O₂-treatment were determined by comet assay. \square , % Fluorescence in tail; \blacklozenge , Inhibitory effect of cell damage. Experiments were performed in triplicate and the data are

expressed as mean \pm SE.

Fig. 1-29. Cytotoxic effects of the active compounds isolated from *E. cava*. The viability of Vero cell was determined by MTT assay. Experiments were performed in triplicate and the data are expressed as mean \pm SE.

Fig. 2-1. Effects of enzymatic extract of *E. cava* on the inhibition activity of LPS-induced NO (nitric oxide) production in RAW264.7 cells. □, 25 ug/ml; ▤, 50 ug/ml; ▥, 100 ug/ml; ■, 200 ug/ml. V; Viscozyme extract, C; Celluclast extract, AMG; AMG extract, T; Termamyl extract, U; Ultraflo extract, P; Protamex extract, K; Kojizyme extract, N; Neutrase extract, F; Flavourzyme extract, A; Alcalase extract, D.W; Distilled water extract. Yield of enzymatic extracts of *E. cava* (%). Experiments were performed in triplicate and the data are expressed as mean \pm SE.

Fig. 2-2. Isolation and purification scheme of the purified polysaccharide from AMG extract of *E. cava*.

Fig. 2-3. The Bio-LC chromatogram for the monosugar composition of the original, >50 kDa Fr, crude polysaccharide (CPS), purified polysaccharide (PPA) of AMG extract from *E. cava*

Fig. 2-4. Calibration curve of dextran standards for the determination of the average molecular weight of the *E. cava* sample. The retention time is plotted against the molecular weight of the dextrans.

Fig. 2-5. Inhibitory effects of molecular weight fractions on LPS-induced NO (nitric oxide) production in RAW264.7 cells. □, 6.25 ug/ml; ▤, 12.5 ug/ml; ▥, 25 ug/ml; ▦, 50 ug/ml; ■, 100 ug/ml. Experiments were performed in triplicate

and the data are expressed as mean \pm SE.

Fig. 2-6. Inhibitory effects of separated fractions (CPS) on LPS-induced NO (nitric oxide) production in RAW264.7 cells. □, 6.25 ug/ml; ▣, 12.5 ug/ml; ▤, 25 ug/ml; ▥, 50 ug/ml; ■, 100 ug/ml. Experiments were performed in triplicate and the data are expressed as mean \pm SE.

Fig. 2-7. Inhibitory effects of PPA on LPS-induced NO (nitric oxide) production in RAW264.7 cells. □, 3.125 ug/ml; ▣, 6.25 ug/ml; ▤, 12.5 ug/ml; ▥, 25 ug/ml; ■, 50 ug/ml. Experiments were performed in triplicate and the data are expressed as mean \pm SE.

Fig. 2-8. Inhibition of inducible nitric oxide synthase (iNOS) protein expression by isolated PPA. RAW 264.7 cells were pretreated with different concentrations of sulfated PPA for 1hr and stimulated with LPS (1 ug/ml) for another 24 hr.

Fig. 2-9. Inhibition of cyclooxygenase-2 protein expression by isolated PPA. RAW 264.7 cells were pretreated with different concentrations of isolated PPA for 1hr and stimulated with LPS (1 ug/ml) for another 24 hr.

Fig. 2-10. Inhibition of isolated PPA on PGE₂ production in RAW 264.7 macrophage cells. PGE₂ production in supernatant fluid was measured using an ELISA kit. Experiments were performed in triplicate and the data are expressed as mean \pm SE.

LIST OF TABLE

- Table 1-1. DPPH radical scavenging activities of fractions separated by organic solvents from ethyl acetate fraction of *Ecklonia cava*
- Table 1-2. ^1H NMR data of pyrogallol-6,6'-bieckol (PYB) in $\text{DMSO-}d_6$ (500 MHz)
- Table 1-3. ^{13}C NMR data of pyrogallol-6,6'-bieckol (PYB) in $\text{DMSO-}d_6$ (100 MHz)
- Table 1-4. ^1H NMR data of 2,7''-phloroglucino-6,6'-bieckol (PHB) in $\text{DMSO-}d_6$ (500 MHz)
- Table 1-5. ^{13}C NMR data of 2,7''-phloroglucino-6,6'-bieckol (PHB) in $\text{DMSO-}d_6$ (100 MHz)
- Table 1-6. ^1H NMR data of phloroglucino-pyrogallol-6,6'-bieckol (PPB) in $\text{DMSO-}d_6$ (500 MHz)
- Table 1-7. ^{13}C NMR data of phloroglucino-pyrogallol-6,6'-bieckol (PPB) in $\text{DMSO-}d_6$ (100 MHz)
- Table 2-1. Approximate monosugar composition of sulfated polysaccharide fraction isolated from AMG extract of *E. cava* separated by molecular weight membrane, ethanol precipitation, and column-chromatography



Part I.
Antioxidant polyphenol compounds
isolated from *Ecklonia cava*

ABSTRACT

In the present study, the polyphenolic compounds have been isolated from *Ecklonia cava* and identified as pyrogallol-6,6'-bieckol (PYB), 6,6'-bieckol (BEK), 2,7''-phloroglucinol-6,6'-bieckol (PHB), and pyrogallol-phloroglucinol-6,6'-bieckol (PPB) by NMR and LC mass spectroscopy. The antioxidant properties of the active compounds were investigated against H₂O₂-induced cell damage. The antioxidant potential of the active compounds were evaluated by several *in vitro* assays such as scavenging activities (DPPH, hydroxyl, alkyl, superoxide radical scavenging assays) by electron spin resonance (ESR) spectrometry, intracellular reactive oxygen species (ROS) scavenging activity (DCFH-DA assay), and DNA damage (comet assay). The active compounds (PYB, BEK, PHB, and PPB) showed strong scavenging activities on DPPH, alkyl, hydroxyl, superoxide radical scavenging (IC₅₀; 0.4, 0.43, 0.5, and 0.88 ug/ml for DPPH, IC₅₀; 1.76, 1.92, 2.02, and 2.48 ug/ml for alkyl, IC₅₀; 39.54, 41.75, 73.68, and 61.30 ug/ml for hydroxyl, IC₅₀; 18.50, 20.27, 55.71, and 166.22 ug/ml for superoxide), respectively. Further, all the active compounds effectively inhibited H₂O₂-induced DNA damage. Hence, these results showed that the active compounds, available in *E. cava* could be used as natural antioxidant agents in food and pharmaceutical industries.

1. Introduction

Reactive oxygen species (ROS) cause extensive oxidative damage to cellular molecules such as DNA, proteins and lipids. Consequently, they contribute to the pathogenesis of oxidative stress-related diseases (Nozik-Grayck and Stenmark, 2007; Kabeya et al., 2008). In recent years, interest in utilizing natural antioxidants has been increased substantially (Heo et al., 2006). Epidemiological studies have also been shown that a higher intake of fresh fruits, vegetables, tea, wine, and algae is associated with reduced ROS-induced diseases (Kooncumchoo et al., 2006). Polyphenols, flavonoids and other non-nutrient compounds of algae, fruits and vegetables have been recognized as potential factors that can be beneficial to human health because of their antioxidant, anticarcinogenic, and anti-inflammatory activities.

Ecklonia cava is a brown alga (Laminariaceae) that is abundant in the subtidal regions of Jeju Island in Korea. Recently, it has been reported that *Ecklonia cava* exhibits radical scavenging activity (Heo et al., 2005; 2008), anti-plasmin inhibitory activity (Fukuyama et al., 1990), anti-mutagenic activity (Lee et al., 1998; Han et al., 2000), anti-bactericidal activity (Nagayama et al., 2002), HIV-1 reverse transcriptase and protease inhibitory activity (Ahn et al., 2004) and tyrosinase inhibitory activity (Heo et al., 2008).

Phlorotannin components, which is oligomeric polyphenol of phloroglucinol unit, are responsible for the biological activities of *Ecklonia cava* and phlorotannins such as PYB, BEK, PHB, and PPB were identified in *Ecklonia cava*. During the investigation of

antioxidative components in *E. cava*, we observed that four active compounds (PYB, BEK, PHB, and PPB) possessed very strong activity.

Therefore this present study was planned to isolate the polyphenolic compound (PYB, BEK, PHB, and PPB) and unravel its antioxidative potential employing in vitro assays: DPPH, hydroxyl, alkyl, superoxide radical scavenging assays, intracellular reactive oxygen species (ROS) scavenging activity (DCFH-DA assay), and DNA damage (comet assay).



2. Materials & Methods

2.1. Chemicals

5,5-Dimethyl-1-pyrroline N-oxide (DMPO), 3-(4,5-Dimethylthiazol-2-yl)-2,5-diphenyltetrazolium bromide (MTT), 2,2-azobis (2-amidinopropane) hydrochloride (AAPH), α -(4-pyridyl-1-oxide)-N-t-butyl nitron (4-POBN), 1,1-diphenyl-2-picrylhydrazyl (DPPH), peroxidase, 2,2-azino-bis(3-ethylbenzthiazoline)-6-sulfonic acid (ABTS), 2',7'-dichlorodihydrofluorescein diacetate (DCFH-DA) were obtained from sigma Chemical Co. (St. Louis, Mo, USA). All other reagents were in analytical grade.

2.2. Plant material

Ecklonia cava was collected along Jeju Island coast of Korea during February and May 2007 (Fig. 1-1). The samples were washed three times with tap water to remove the salt, epiphytes, and sand attached to the surface, then carefully rinsed with fresh water, and maintained in a medical refrigerator at -20 °C. Thereafter, the frozen samples were lyophilized and homogenized with a grinder prior to extraction.



Fig.1-1. The photograph of a brown alga, *Ecklonia cava*.

2.3. Extraction and isolation

The dried *E. cava* powder (500g) was extracted by using 80 % aqueous methanol (5 L × 3) at room temperature for a week. The liquid layer was obtained by filtration, and the filtrate was concentrated using evaporator under reduced pressure. Water was added to the extract, and then the aqueous layer was partitioned with ethyl acetate (EtOAc). The EtOAc extract (45.65 g) was mixed with celite. The mixed celite was dried and packed into a glass column, and eluted in the order of hexane, methylene chloride, diethyl ether, and methanol. The diethyl ether fraction (26.69 g) was subjected to Sephadex LH-20 column chromatography using stepwise gradient with chloroform/methanol (2/1→0/1) to give 8 fractions. The fraction 5 (8.7g) was further purified by HPLC to give PYB (Pyrogallol-6,6'-bieckol), BEK (6,6'-bieckol). The fraction 7 (1.7g) was also purified by HPLC to give PHB (2,7''-phloroglucinol-6,6'-bieckol), PPB (Phloroglucinol-pyrogallol-6,6'-bieckol) (Fig. 1-2).

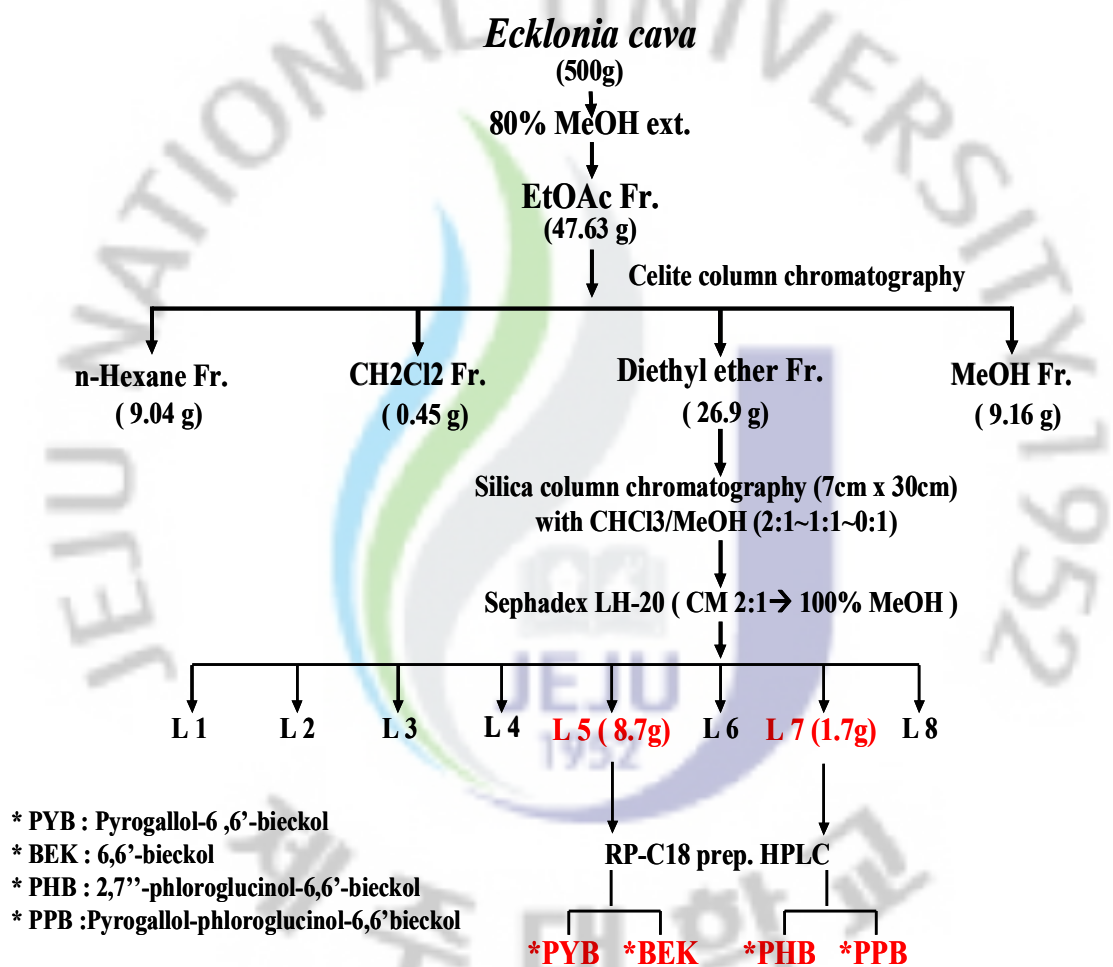


Fig.1-2. Isolation and purification scheme of the active compounds from *E. cava*.

2.4. DPPH radical scavenging assay

The DPPH radical scavenging activity was evaluated by ESR spectrometer (JES-FA machine, JOEL, Tokyo, Japan) according to the method described by Nanjo et al. (1996). 60 μ l of each extract was added to 60 μ l of DPPH (10 μ mol/l) in ethanol. After 10 seconds of vigorous mixing, the solutions were transferred to Teflon capillary tubes and fitted into the cavity of the ESR spectrometer exactly 2 min later under the following measurement conditions : central field 3475 G, modulation frequency 100 kHz, modulation amplitude 2 G, microwave power 5 mW, gain 6.3×10^5 , and temperature 25°C. All the radical scavenging activities (%) were calculated by using the following equation, in which H and H₀ were the relative peak heights of the radical signals with and without a sample, respectively.

$$\text{Radical scavenging activity} = [1 - (H / H_0) \times 100]$$

2.5. Alkyl radical scavenging assay

Alkyl radicals were generated via AAPH. The reaction mixture containing 10 mmol/l AAPH and 10 mmol/l 4-POBN were mixed with the tested compounds. The solutions were incubated for 30 min at 37°C in a water bath and then transferred to Teflon capillary tubes (Hiramoto et al., 1993). The spin adduct was recorded using a JES-FA ESR spectrometer under the following measurement conditions : central field 3475 G, modulation frequency 100 kHz, modulation amplitude 2 G, microwave power 10 mW, gain 6.3×10^5 , and temperature 25°C. The radical scavenging activity (%) was presented as described in the section 2.4.

2.6. Hydroxyl radical scavenging assay

Hydroxyl radical were generated via a Fenton reaction, and reacted rapidly with nitron spin trap DMPO. The resultant DMPO-OH adducts was detected using an ESR spectrometer (Rosen and Rauckman, 1984). Reaction mixtures containing 100 μ l of 0.3 M DMPO, 100 μ l of 10 mM FeSO₄, and 100 μ l of 10 mM H₂O₂ were mixed with the test compounds, then transferred to Teflon capillary tube. The spin adducts was measured by ESR spectrometer exactly 2.5 min later under the following measurement conditions : central field 3475 G, modulation frequency 100 kHz, modulation amplitude 2 G, microwave power 1 mW, gain 6.3×10^5 , and temperature 25 °C. The hydroxyl radical scavenging activity (%) was presented as described in the section 2.4.

2.7. Superoxide radical assay

Superoxide radical was generated by UV irradiation of a riboflavin/EDTA solution. The reaction mixture containing 0.8 mM riboflavin, 1.6 mM EDTA, 0.8 M DMPO, and various concentrations of compounds were irradiated for 1 min under UV lamp at 365 nm. The mixtures were transferred to Teflon capillary tube and spin adduct were measured by ESR spectrometer. Experimental conditions were as follows: magnetic field, 336.5 ± 5 mT; power, 10 mW; modulation frequency, 9.41 GHz; amplitude, $1 \cdot 1000$; sweep time, 1 min.

2.8. Antioxidant activities by Vero cell lines

2.8.1. Cell culture

The monkey kidney fibroblast cell line (Vero) was maintained at 37 °C in an incubator with humidified atmosphere of 5 % CO₂. Cells were cultured in Dulbecco's modified Egel's medium containing 10 % heat-inactivated fetal bovine serum, streptomycin (100 ug/ml), and penicillin (100 unit/ml).

2.8.2. Intracellular reactive oxygen species (ROS) measurement

For the detection of intracellular ROS, Vero cells were seeded in 96-well plates at a concentration of 1×10^5 cells/ml. After 16 hr, the cells were treated with various concentrations of the compounds, and incubated at 37 °C under a humidified atmosphere. After 30 min, H₂O₂ was added as a final concentration of 1 mM, and then cells were incubated for an additional 30 min at 37 °C. Finally, 2',7'-dichlorodihydrofluorescein diacetate (DCFH-DA; 5 ug/ml) was introduced to the cells, and 2',7'-dichlorodihydrofluorescein fluorescence was detected at an excitation wavelength of 485 nm and an emission wavelength of 535 nm, using a Perkin-Elmer LS-5B spectrofluorometer. The percentage of H₂O₂ scavenging activity was calculated in according to the following equation:

$$\text{H}_2\text{O}_2 \text{ scavenging activity (\%)} = (1 - (C1 / C0)) \times 100$$

Where C1 is the fluorescence intensity of cells treated with H₂O₂ and compounds, and C0 is the fluorescence intensity of cells treated with H₂O₂ and distilled water of compounds.

2.8.3. Assessment of cell cytotoxicity

Cell cytotoxicity was estimated via MTT assay, which is a test of metabolic competence predicated upon the assessment of mitochondrial performance. It is a colorimetric assay, which is dependent on the conversion of yellow tetrazolium bromide to its purple formazan derivative by mitochondrial succinate dehydrogenase in viable cells (Mosmann, 1983). Vero cells were seeded in 96-well plate at a concentration of 1×10^5 cells/ml. After 16 hr, the cells were treated with compounds at different concentrations, and then cells were incubated for 24 hr at 37 °C. MTT stock solution (50 μ l; 2 mg/ml) was then applied to the wells to a total reaction volume of 250 μ l. After 4 hr of incubation, the plates were centrifuged for 5 min at 800 \times g, and the supernatants were aspirated. The formazan crystals in each well were dissolved in 150 μ l of dimethylsulfoxide (DMSO), and the absorbance was measured via ELISA at a wavelength of 540 nm. Relative cell cytotoxicity was evaluated in accordance with the quantity of MTT converted to the insoluble formazan salt. The optical density of the formazan generated in the control cells was considered to represent 100 % viability. The data were expressed as mean percentage of the viable cells versus the respective control.

2.8.4. Comet assay

Comet assay was performed to assess oxidative DNA damage. The cell pellet (1.5×10^5 cells) was mixed with 100 μ l of 0.5% low melting point agarose (LMPA) at 39 °C and spread on a fully frosted microscopic slide that was pre-coated with 200 μ l of 1% normal melting point agarose (NMPA). After solidification of the agarose, the slide was covered with another 100 μ l of 0.5% LMPA and then immersed in lysis solution (2.5 M

NaCl, 100 mM Na-EDTA, 10 mM Tris, 1% Trion X-100, and 10% DMSO, pH 10) for 1 hr at 4 °C. The slides were then placed in a buffer containing 300 mM NaOH and 10 mM Na-EDTA (pH 13) for 60 min to allow DNA unwinding and the expression of the alkali labile damage. An electrical field was applied (300 mA, 25 V) for 20 min at 4 °C to draw negatively charged DNA toward an anode. After electrophoresis, the slides were washed three times with neutralizing buffer (0.4 M Tris, pH 7.5) for 5 min at 4 °C and then stained with 50 ul of ethidium bromide (20 ug/ml). The slides were observed by using fluorescence microscope and image analysis (Kinetic Imaging, Komet 5.5, UK). The percentage of total fluorescence in the tail and the tail length of the 50 cells/slide were recorded.

2.9. Statistical analysis

Data were analyzed using the SPSS package for windows (version 10). Values were expressed as mean \pm standard error (SE). The mean values of the tail intensity from each treatment were compared using one-way analysis of variance (ANOVA) followed by Duncan's multiple range test. P-value of less than 0.05 was considered significant.

3. RESULT

3.1 Isolation and purification of active compounds

In the preliminary studies, we have found that the *Ecklonia cava* exhibited prominent radical scavenging activity in EtOAc fraction. The EtOAc fraction was mixed celite. The mixed celite was dried and packed into a glass column, and eluted in the order hexane, dichloro methane, diethyl ether, and methanol successively. As shown in the Table 1, the diethyl ether fraction showed the most DPPH radical scavenging activity than any other fractions.

Table 1-1. DPPH radical scavenging activities of fractions separated by organic solvents from ethyl acetate fraction of *Ecklonia cava*

n-hexane fraction	Dichloro methane fraction	Diethyl ether fraction	Methanol fraction
31.1 %	48.3 %	64.1 %	55.9 %

The diethyl ether fraction was subjected to sephadex LH-20 chromatography with a chloroform-methanol gradient system (2:1 to 100% methanol) to provide 8 fractions. As shown in the Fig. 1-3, five fractions (L 3, 4, 5, 6, and 7) showed strong DPPH radical scavenging activities. And then finally purified by reversed-phase HPLC to give compound (Eckol and Phloroglucinol (L3 fr.), Triphlorethol-A and Eckstolonol (L4 fr.), Dieckol (L6 fr., data not shown) PYB and BEK (L5 fr), PHB and PPB (L7 fr) (Fig. 1-2).

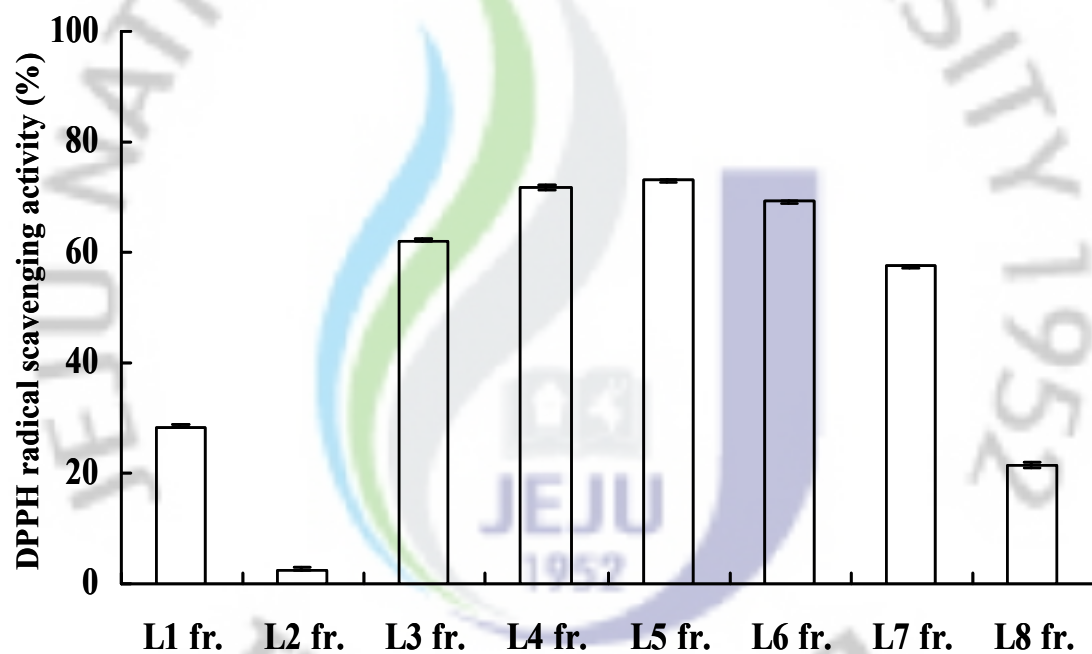


Fig. 1-3. DPPH radical scavenging activities of fractions separated by sephadex LH-20 chromatography from diethyl ether fraction. Experiments were performed in triplicate and the data are expressed as mean \pm SE.

Compound BEK was identified as the known compound 6,6'-bieckol (Fig. 1-4.) by comparison of the LC-mass (Fig. 1-5), ^1H and ^{13}C NMR data (Fig. 1-6.), and the specific rotation value (Murat Artan et al., 2008).

Compound BEK, 6,6'-bieckol: light brown powder (lyophilized); ^1H NMR (DMSO- d_6 , 400 MHz) δ 9.29 (1H, s, OH-9), 9.16 (2H, s, OH-30, 50), 9.15 (1H, s, OH-2), 9.09 (1H, s, OH-4), 8.65 (1H, s, OH-7), 6.09 (1H, s, H-3), 6.05 (1H, s, H-8), 5.80 (1H, d, $J = 2.2$ Hz, H-40), 5.75 (2H, d, $J = 2.2$ Hz, H-20, 60); ^{13}C NMR (DMSO- d_6 , 100 MHz) δ 123.5 (s, C-1), 145.4 (s, C-2), 97.7 (d, C-3), 141.4 (s, C-4), 121.9 (s, C-4a), 141.3 (s, C-5a), 99.7 (d, C-6), 151.3 (s, C-7), 97.8 (d, C-8), 144.5 (s, C-9), 122.7 (s, C-9a), 137.2 (s, C-10a), 160.4 (s, C-10), 93.7 (d, C-20), 158.8 (s, C-30), 96.1 (d, C-40), 158.8 (s, C-50), 93.7 (d, C-60); LREIMS m/z 742.10 $[\text{M}]^+$.

Compound PYB, pyrogallol-6,6'-bieckol (Fig. 1-7) was obtained as an amorphous, brown powder, with a molecular formula of $\text{C}_{42}\text{H}_{26}\text{O}_{21}$ determined by FABMS (m/z found 889.3 $[\text{M} + \text{Na}]^+$) (Fig. 1-8), and this was supported by the ^1H and ^{13}C , and DEPT NMR data (Table 1-2, 3, Fig. 1-9).

Compound PHB, 2,7''-phloroglucinol-6,6'-bieckol (Fig. 1-10) was obtained as an amorphous, brown powder, with a molecular formula of $\text{C}_{48}\text{H}_{30}\text{O}_{23}$ determined by FABMS (m/z found 997.2 $[\text{M} + \text{Na}]^+$, m/z found 975.1 $[\text{M} + \text{H}]^+$) (Fig. 1-11), and this was supported by the ^1H and ^{13}C , and DEPT NMR data (Table 1-4, 5, Fig. 1-12).

Compound PPB, phloroglucinol-pyrogallol-6,6'-bieckol (Fig. 1-13) was obtained as an amorphous, brown powder, with a molecular formula of $\text{C}_{48}\text{H}_{30}\text{O}_{23}$ determined by FABMS (m/z found 997.3 $[\text{M} + \text{Na}]^+$, m/z found 975.2 $[\text{M} + \text{H}]^+$) (Fig. 1-14), and this was supported by the ^1H and ^{13}C , and DEPT NMR data (Table 1-6, 7, Fig. 1-15).

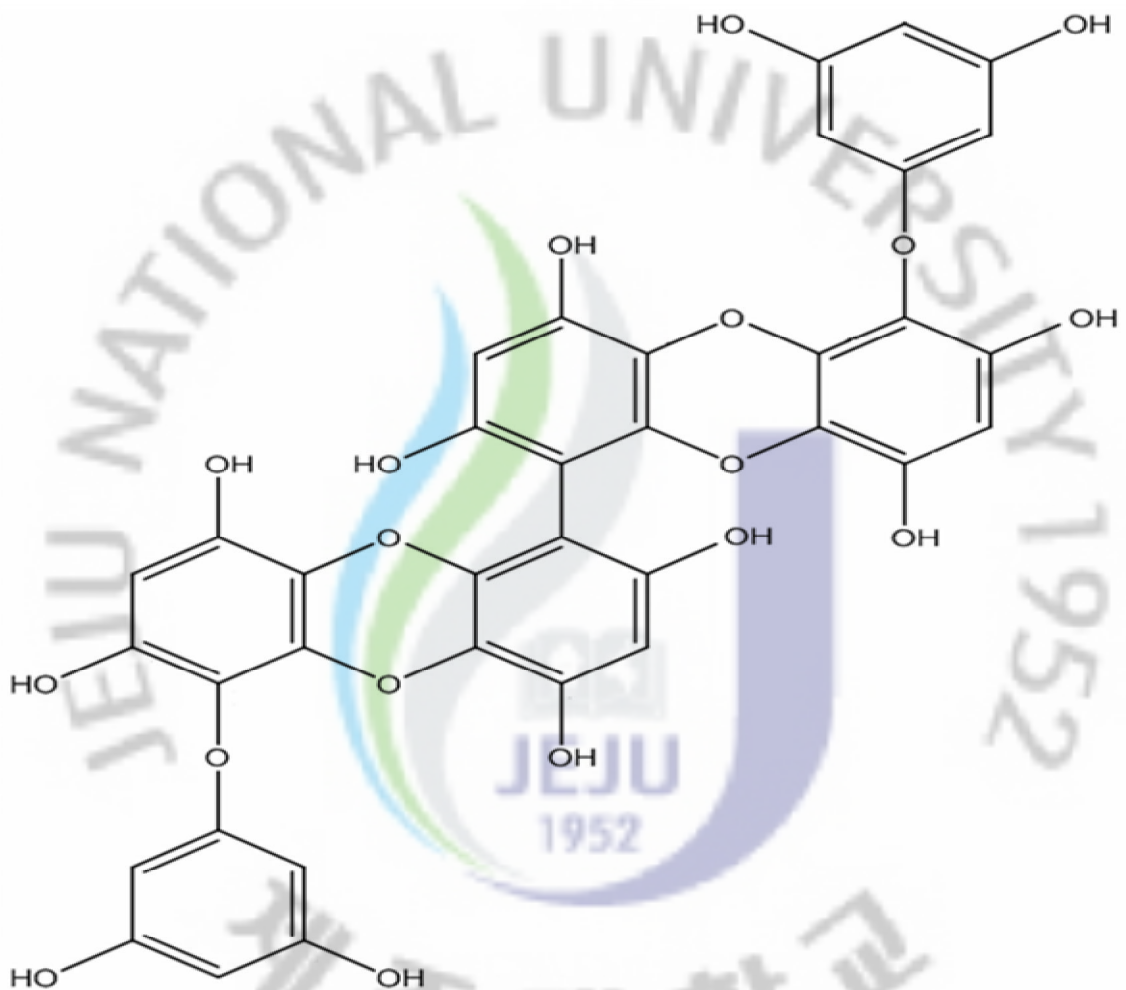


Fig. 1-4. Chemical structure of the 6,6'-bieckol (BEK) isolated *E. cava*.

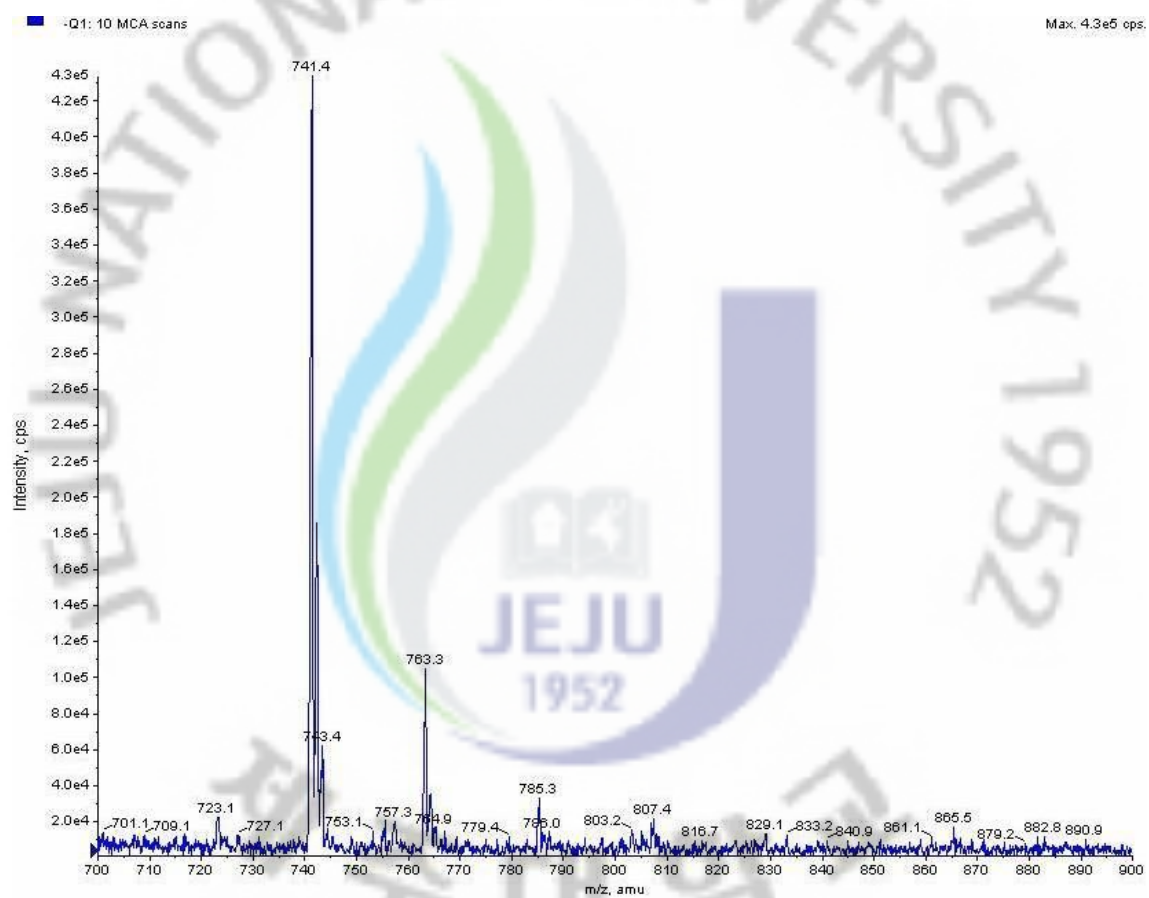


Fig. 1-5. The LC-mass spectrum of 6,6'-bieckol (BEK) isolated from *E. cava*.

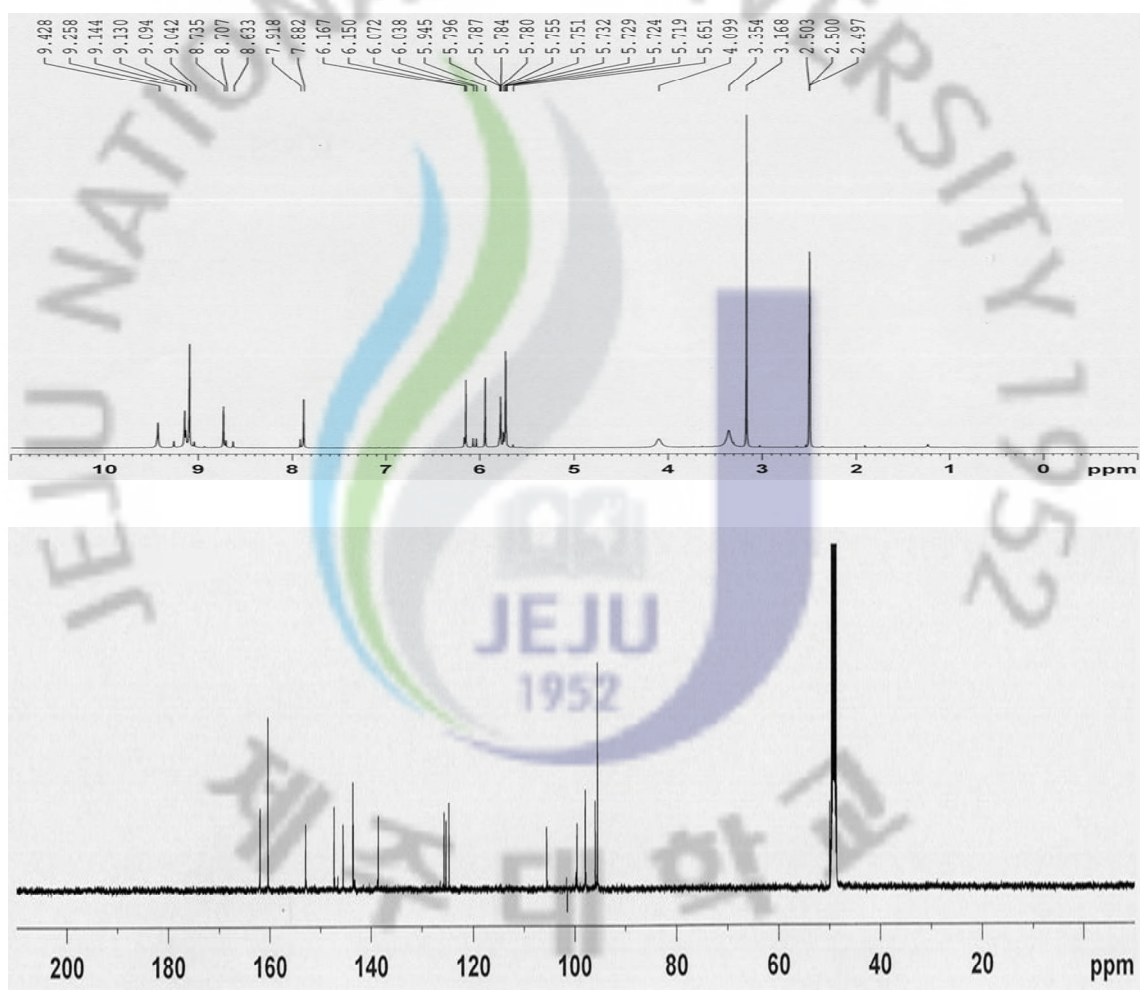
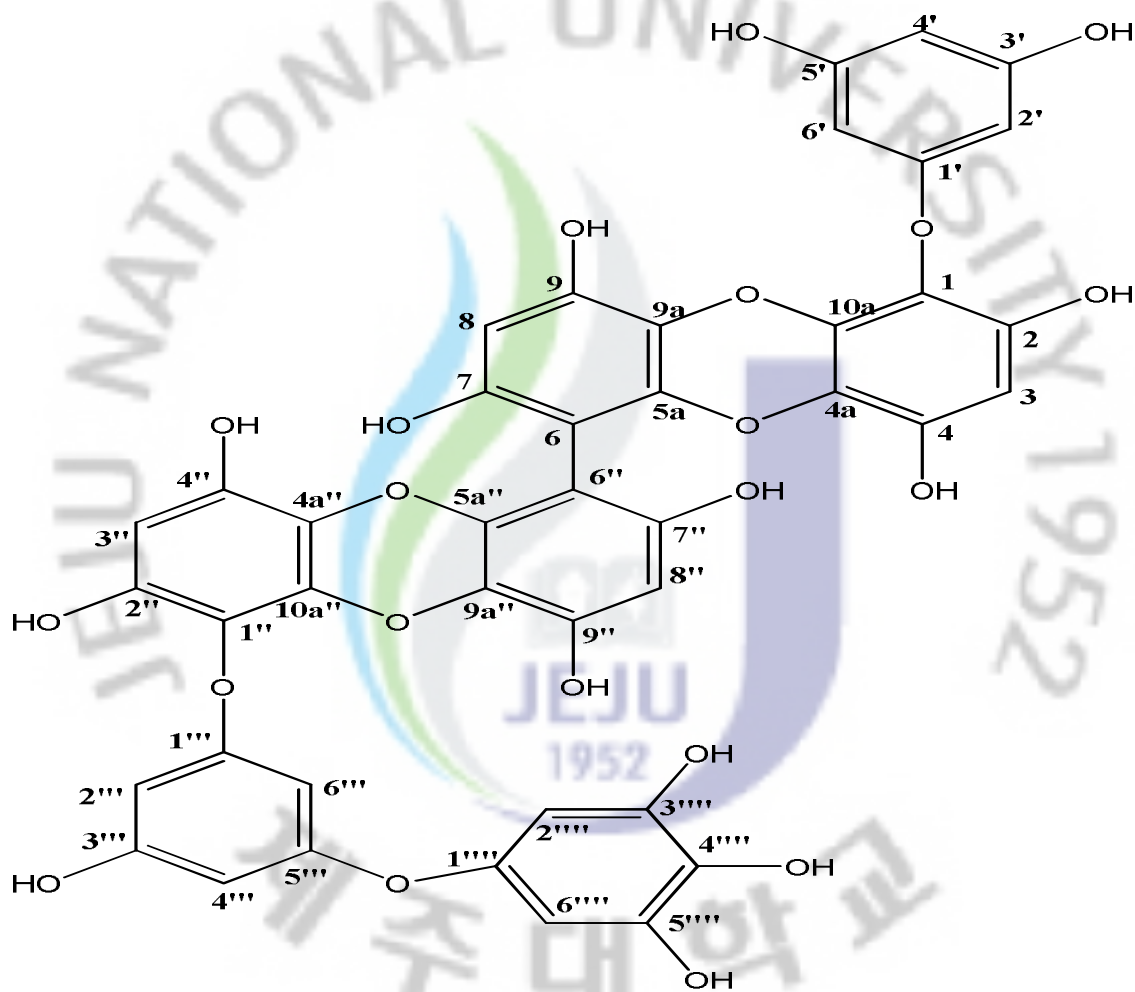


Fig. 1-6. Proton and Carbon NMR spectrum of 6,6'-bieckol (BEK).



6-(3,5-dihydroxyphenoxy)-6'-(3-hydroxy-5-(3,4,5-trihydroxyphenoxy)phenoxy)-1,1'-bidibenzo[b,e][1,4]dioxin-2,2',4,4',7,7',9,9'-octaol

Fig. 1-7. Chemical structure of the pyrogallol-6,6'-bieckol (PYB) isolated *E. cava*.

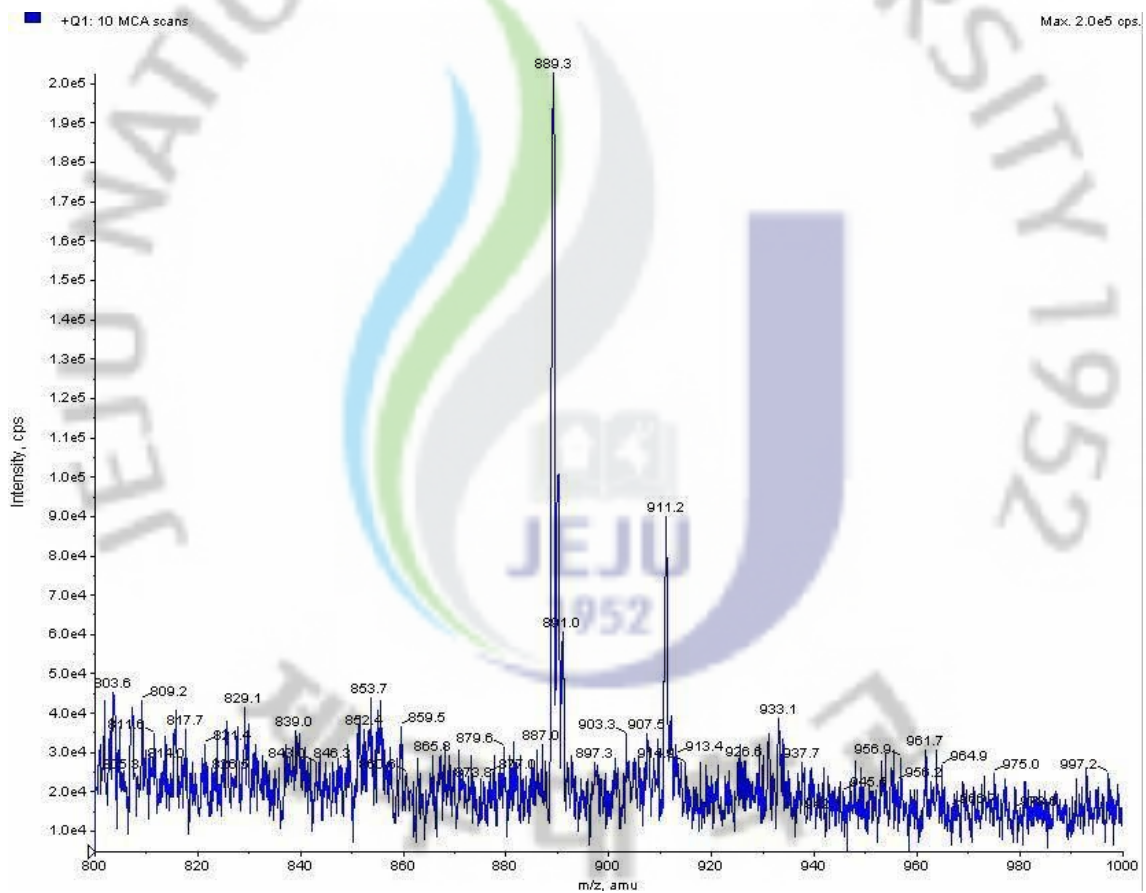


Fig. 1-8. The LC-mass spectrum of pyrogallol-6,6'-bieckol (PYB) isolated form *E. cava*.

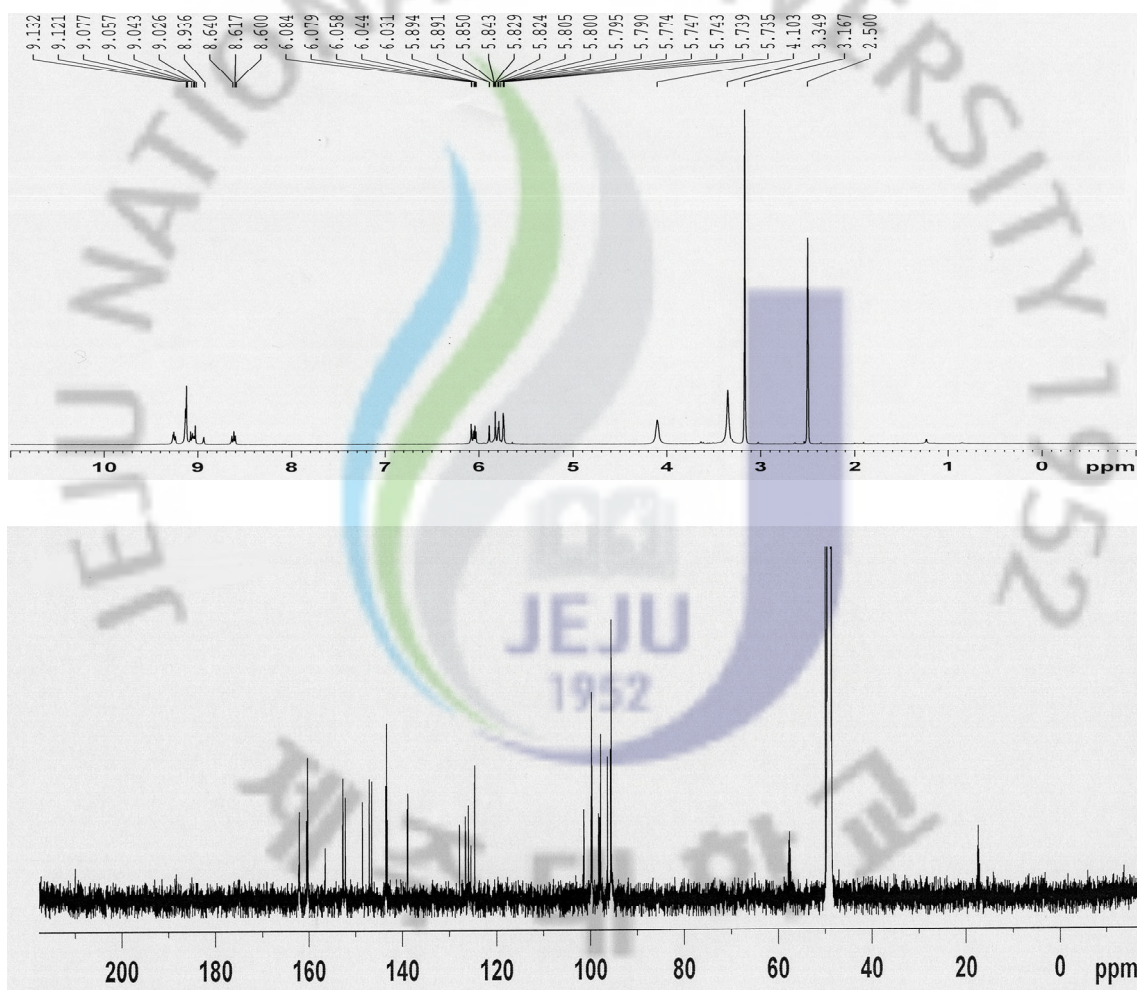


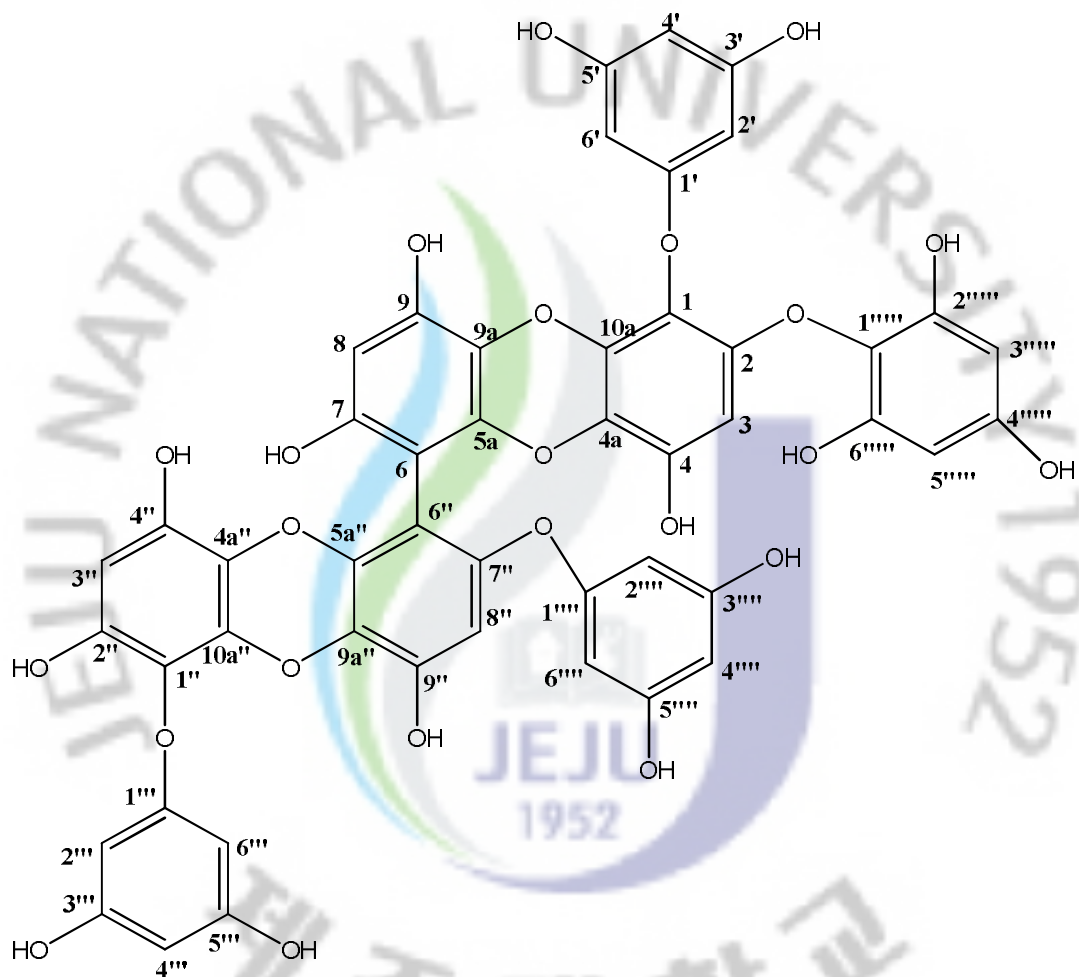
Fig. 1-9. Proton and Carbon NMR spectrum of pyrogallol-6,6'-bieckol (PYB).

Table 1-2. ¹H NMR data of Pyrogallol-6,6'-bieckol (PYB) in DMSO-*d*₆ (500 MHz)

Position (C [#])	δ_{H} (mult, J)	Position (C [#])	δ_{H} (mult, J)
3	6.04 (1H, s)	4-OH	9.04 (1H, s)
8	6.04 (1H, s)	7-OH	8.94 (1H, s)
2'	5.74 (1H, m)	3'-OH	9.12 (1H, s)
4'	5.79 (1H, m)	5'-OH	9.12 (1H, s)
6'	5.74 (1H, m)	2''-OH	9.08 (1H, s)
3''	6.05 (1H, s)	4''-OH	9.03 (1H, s)
8''	6.03 (1H, s)	7''-OH	8.64 (1H, s)
2'''	5.89 (1H, d, <i>J</i> = 2.2 Hz)	9''-OH	9.25 (1H, s)
4'''	5.89 (1H, d, <i>J</i> = 2.2 Hz)	3'''-OH	9.13 (1H, s)
6'''	5.82 (1H, d, <i>J</i> = 2.2 Hz)	3''''-OH	8.62 (1H, s)
2''''	6.08 (1H, d, <i>J</i> = 2.01 Hz)	4''''-OH	9.24 (1H, s)
6''''	6.08 (1H, d, <i>J</i> = 2.01 Hz)	5''''-OH	8.60 (1H, s)
2-OH	9.06 (1H, s)		

Table 1-3. ^{13}C NMR data of Pyrogallol-6,6'-bieckol (PYB) in $\text{DMSO-}d_6$ (100 MHz)

Position (C [#])	δ_c (mult)	Position (C [#])	δ_c (mult)
1	126.2 (s)	4''	143.5 (s)
2	143.2 (s)	4a''	126.9 (s)
3	95.5 (d)	5''	
4	143.4 (s)	5a''	147.1 (s)
4a	126.0 (s)	6''	101.4 (s)
5		7''	152.3 (s)
5a	147.2 (s)	8''	96.4 (d)
6	101.3 (s)	9''	152.7 (s)
7	148.6 (s)	9a''	126.6 (s)
8	97.8 (d)	10''	
9	152.3 (s)	10a''	139.0 (s)
9a	126.7 (s)	1'''	160.4 (s)
10		2'''	99.6 (d)
10a	138.8 (s)	3'''	156.6 (s)
1'	162.3 (s)	4'''	99.7 (d)
2'	98.3 (d)	5'''	160.6 (s)
3'	162.1 (s)	6'''	97.8 (d)
4'	95.5 (d)	1''''	152.8 (s)
5'	162.2 (s)	2''''	99.9 (d)
6'	98.1 (d)	3''''	146.61 (s)
1''	125.5 (s)	4''''	127.9 (s)
2''	143.6 (s)	5''''	146.58 (s)
3''	95.7 (d)	6''''	99.8 (d)



2',6,6'-tris(3,5-dihydroxyphenoxy)-7-(2,4,6-trihydroxyphenoxy)-1,1'-bidibenzo[b,e][1,4]dioxine-2,4,4',7',9,9'-hexaoal

Fig. 1-10. Chemical structure of the 2,7''-phloroglucinol-6,6'-bieckol (PHB) isolated *E. cava*.

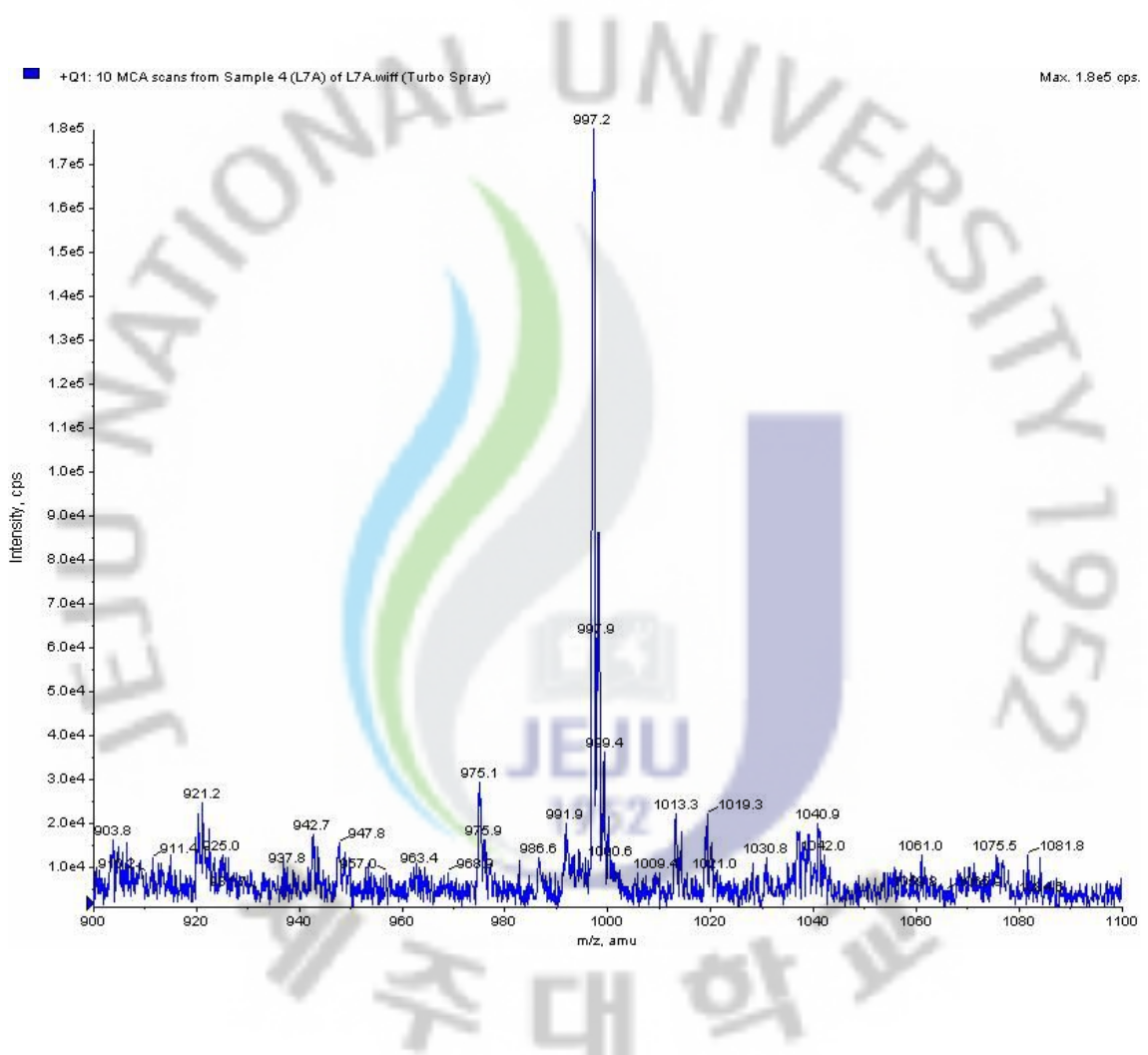


Fig. 1-11. The LC mass spectrum of 2,7''-phloroglucinol-6,6'-bieckol (PHB) isolated from *E. cava*

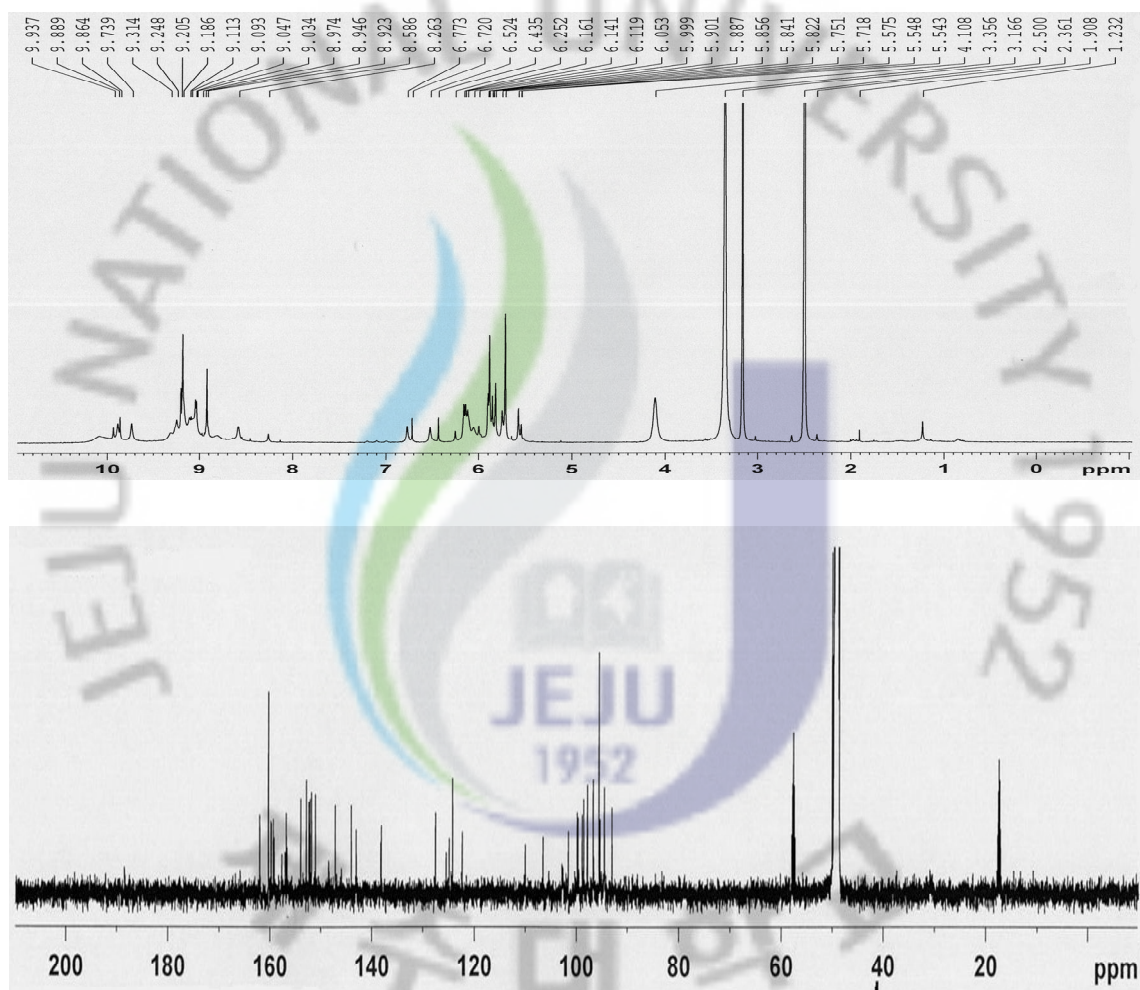


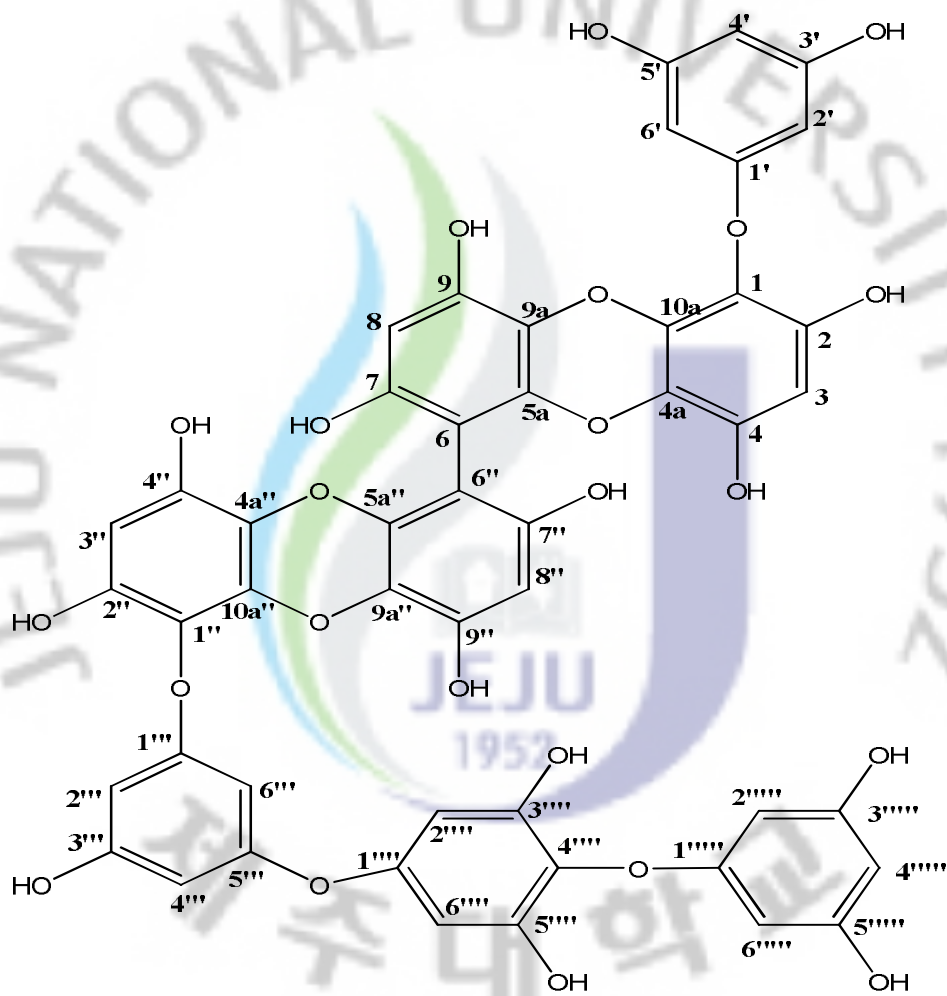
Fig. 1-12. Proton and Carbon NMR spectrum of 2,7''-phloroglucinol-6,6'-bieckol (PHB).

Table 1-4. ¹H NMR data of 2,7''-phloroglucino-6,6'-bieckol (PHB) in DMSO-*d*₆ (500 MHz)

Position (C [#])	δ_{H} (<i>mult, J</i>)	Position (C [#])	δ_{H} (<i>mult, J</i>)
3	5.57 (1H, s)	4-OH	8.93 (1H, s)
8	5.89 (1H, s)	7-OH	8.93 (1H, s)
2'	5.74 (1H, m)	3'-OH	9.19 (1H, s)
4'	5.84 (1H, m)	5'-OH	9.19 (1H, s)
6'	5.74 (1H, m)	2''-OH	9.19 (1H, s)
3''	6.25 (1H, s)	4''-OH	9.04 (1H, s)
8''	6.14 (1H, s)	9''-OH	8.26 (1H, s)
2'''	5.84 (1H, m)	3'''-OH	9.94 (1H, s)
4'''	5.89 (1H, m)	5'''-OH	8.59 (1H, s)
6'''	5.84 (1H, m)	3''''-OH	9.88 (1H, s)
2''''	6.52 (1H, s)	5''''-OH	9.86 (1H, s)
4''''	6.14 (1H, m)	2''''-OH	9.25 (1H, s)
6''''	6.44 (1H, m)	4''''-OH	9.75 (1H, s)
3'''''	6.77 (1H, s)	6''''-OH	9.21 (1H, s)
5'''''	6.72 (1H, s)		

Table 1-5. ^{13}C NMR data of 2,7''-phloroglucinol-6,6''-bieckol (PHB) in $\text{DMSO-}d_6$ (100 MHz)

Position (C [#])	δ_c (mult)	Position (C [#])	δ_c (mult)
1	127.6 (s)	5a''	147.2 (s)
2	143.0 (s)	6''	110.0 (s)
3	93.0 (d)	7''	144.1 (s)
4	137.1 (s)	8''	101.5 (d)
4a	125.6 (s)	9''	151.8 (s)
5		9a''	137.2 (s)
5a	147.2 (s)	10''	
6	106.5 (s)	10a''	144.1 (s)
7	152.2 (s)	1'''	159.7 (s)
8	95.5 (d)	2'''	96.7 (s)
9	152.4 (s)	3'''	157.1 (s)
9a	127.6 (s)	4'''	95.5 (d)
10		5'''	157.1 (s)
10a	137.1 (s)	6'''	96.7 (d)
1'	162.0 (s)	1''''	159.8 (s)
2'	98.7 (d)	2''''	97.8 (d)
3'	160.3 (s)	3''''	159.3 (s)
4'	95.5 (d)	4''''	95.2 (s)
5'	160.3 (s)	5''''	159.2 (s)
6'	98.8 (d)	6''''	97.9 (d)
1''	124.3 (s)	1'''''	122.5 (s)
2''	147.2 (s)	2'''''	153.9 (d)
3''	94.5 (d)	3'''''	99.8 (s)
4''	144.1 (s)	4'''''	156.8 (d)
4a''	124.3 (s)	5'''''	99.9 (s)
5''		6'''''	152.8 (d)



6-(3,5-dihydroxyphenoxy)-6'-(3-(4-(3,5-dihydroxyphenoxy)-3,5-dihydroxyphenoxy)-5-hydroxyphenoxy)-1,1'-bidibenzo[*b,e*][1,4]dioxin-2,2',4,4',7,7',9,9'-octaol

Fig. 1-13. Chemical structure of the phloroglucinol-pyrogallol-6,6'-bieckol (PPB) isolated *E. cava*.

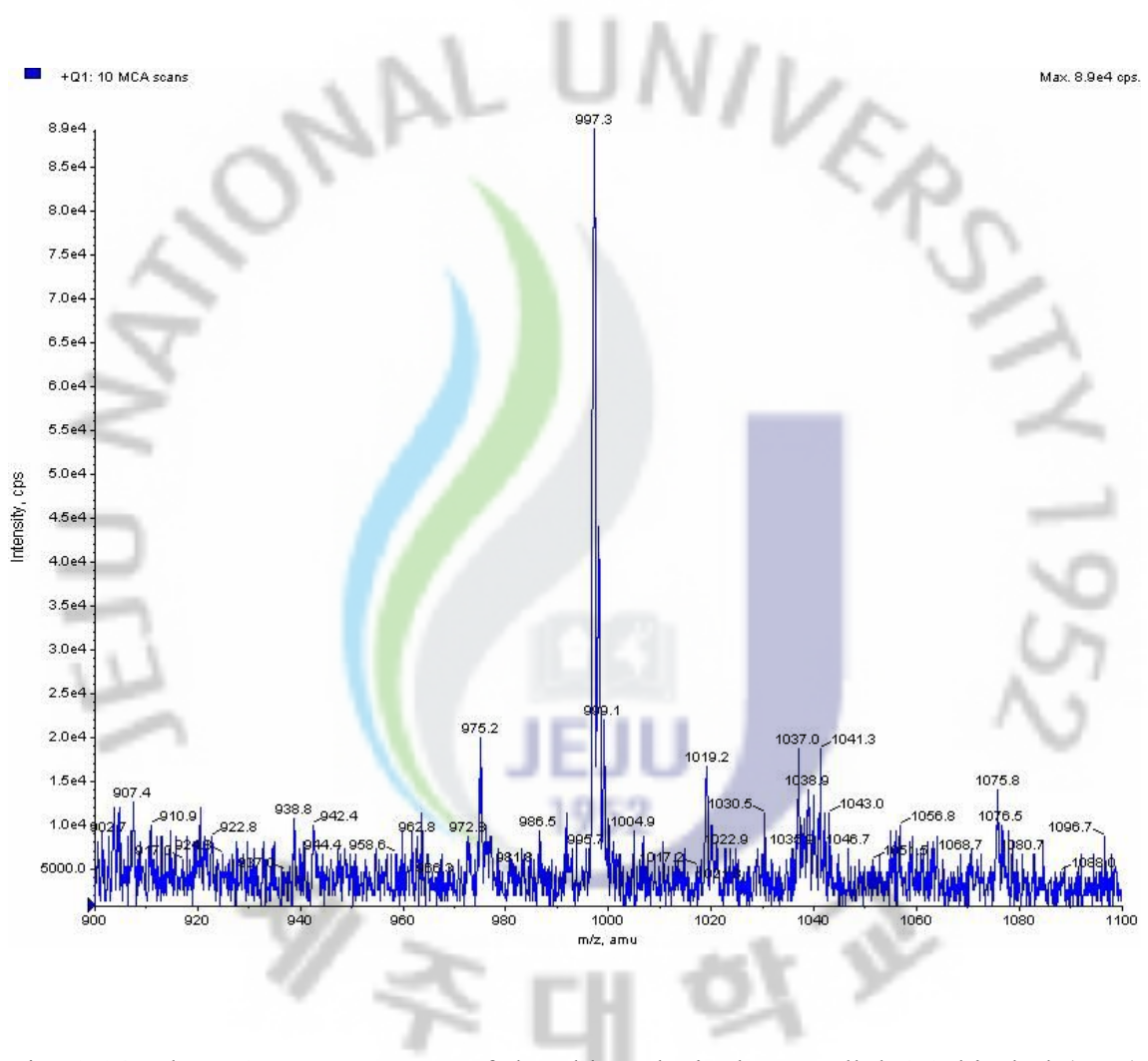


Fig. 1-14. The LC mass spectrum of the phloroglucinol-pyrogallol-6,6'-bieckol (PPB) isolated from *E. cava*

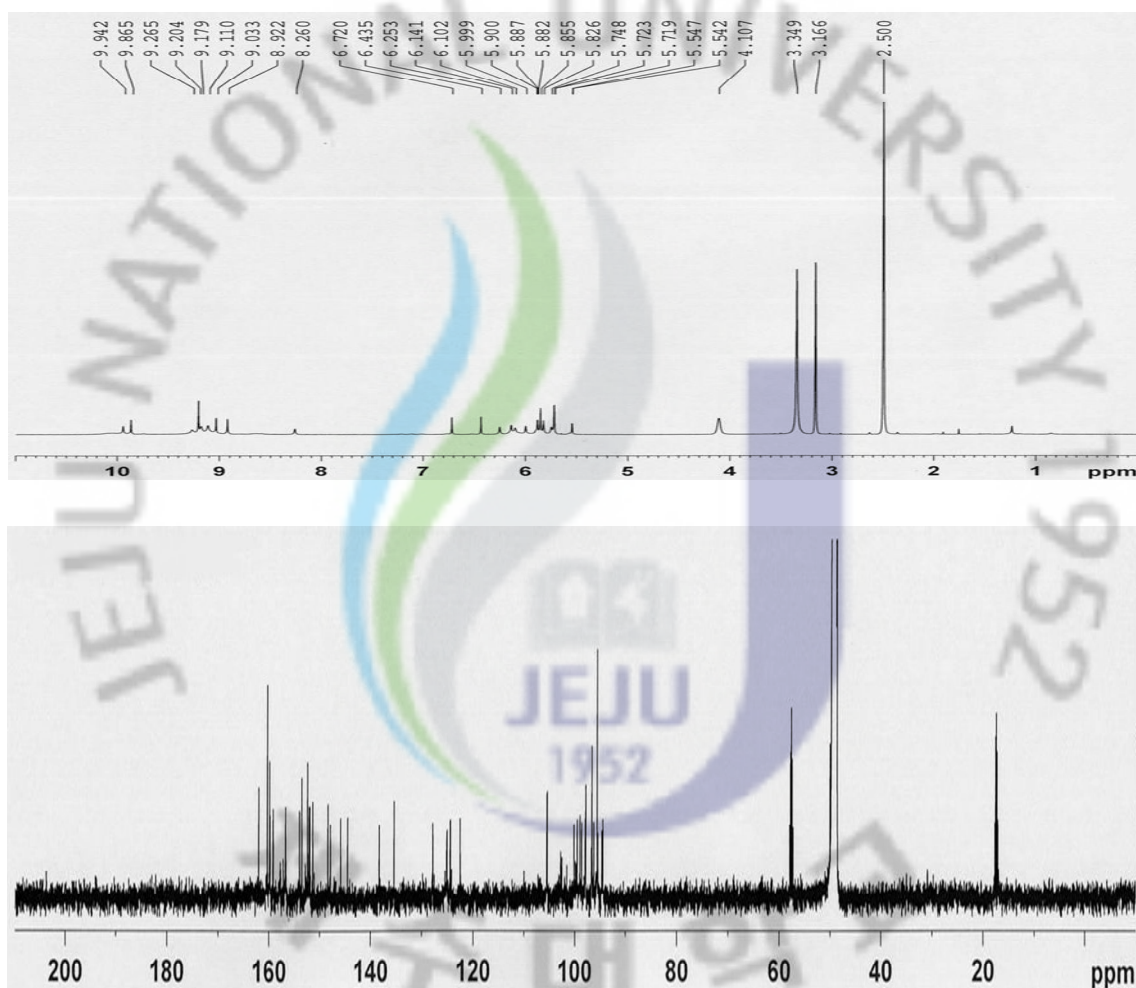


Fig. 1-15. Proton and Carbon NMR spectrum of phloroglucinol-pyrogallol-6,6'-bieckol (PPB).

Table 1-6. ¹H NMR data of phloroglucino-pyrogallol-6,6'-bieckol (PPB) in DMSO-*d*₆ (500 MHz)

Position (C [#])	δ_{H} (<i>mult, J</i>)	Position (C [#])	δ_{H} (<i>mult, J</i>)
3	6.10 (1H, s)	2-OH	9.116 (1H, s)
8	5.99 (1H, s)	4-OH	9.03 (1H, s)
2'	5.72 (1H, m)	7-OH	8.92 (1H, s)
4'	5.75 (1H, m)	9-OH	9.27 (1H, s)
6'	5.72 (1H, m)	3'-OH	9.20 (1H, s)
3''	6.25 (1H, s)	5'-OH	9.20 (1H, s)
8''	6.14 (1H, s)	2''-OH	9.18 (1H, s)
2'''	5.88 (1H, d, <i>J</i> = 2.21 Hz)	4''-OH	9.03 (1H, s)
4'''	5.88 (1H, d, <i>J</i> = 2.21 Hz)	7''-OH	8.92 (1H, s)
6'''	5.85 (1H, d, <i>J</i> = 2.21 Hz)	9''-OH	8.25 (1H, s)
2''''	6.72 (1H, d, <i>J</i> = 2.2 Hz)	3'''-OH	9.94 (1H, s)
6''''	6.08 (1H, d, <i>J</i> = 2.2 Hz)	3''''-OH	9.87 (1H, s)
2'''''	5.89 (1H, d, <i>J</i> = 2.01 Hz)	5''''-OH	9.87 (1H, s)
4'''''	5.54 (1H, d, <i>J</i> = 2.01 Hz)	3'''''-OH	9.20 (1H, s)
6'''''	5.89 (1H, d, <i>J</i> = 2.01 Hz)	5'''''-OH	9.20 (1H, s)

Table 1-7. ^{13}C NMR data of phloroglucinol-pyrogallol-6,6'-bieckol (PPB) in $\text{DMSO-}d_6$
(100 MHz)

Position (C [#])	δ_c (mult)	Position (C [#])	δ_c (mult)
1	125.2 (s)	5a''	147.9 (s)
2	145.9 (s)	6''	105.4 (s)
3	95.5 (d)	7''	148.4 (s)
4	145.9 (s)	8''	95.5 (d)
4a	125.1 (s)	9''	151.4 (s)
5		9a''	127.8 (s)
5a	147.9 (s)	10''	
6	105.5 (s)	10a''	138.3 (s)
7	148.4 (s)	1'''	159.2 (s)
8	95.4 (d)	2'''	100.2 (s)
9	151.9 (s)	3'''	156.9 (s)
9a	127.8 (s)	4'''	99.5 (d)
10		5'''	159.3 (s)
10a	135.3 (s)	6'''	96.3 (d)
1'	161.9 (s)	1''''	154.0 (s)
2'	97.9 (d)	2''''	96.6 (d)
3'	160.3 (s)	3''''	152.1 (s)
4'	95.5 (d)	4''''	122.5 (s)
5'	160.3 (s)	5''''	153.5 (s)
6'	97.8 (d)	6''''	96.6 (d)
1''	124.4 (s)	1'''''	159.9 (s)
2''	144.4 (s)	2'''''	99.0 (d)
3''	94.4 (d)	3'''''	159.8 (s)
4''	144.4 (s)	4'''''	94.6 (d)
4a''	124.5 (s)	5'''''	159.8 (s)
5''		6'''''	98.6 (d)

3.2 DPPH radical scavenging assay

Antioxidant activity of active compounds isolated from *E. cava* was tested for DPPH free radical by ESR technique. DPPH is a stable free radical donor that is widely used to investigate the free radical scavenging effect of natural antioxidant.

The scavenging activities of active compounds on DPPH free radicals are shown in Fig. 1-16. Among the four compounds, PYB showed the highest IC_{50} value for DPPH radical scavenging activity ($IC_{50}=0.4$ ug/ml) and the IC_{50} value of the fractions BEK, PYB, and PPB were 0.43, 0.5, and 0.88 ug/ml, respectively, and radical scavenging activity was dose-dependent. The decreased ESR signal was observed with the activity increment of the fractions (Fig. 1-16). Therefore, the active compounds isolated from *E. cava* would appear to be a potential DPPH free radical scavenger.

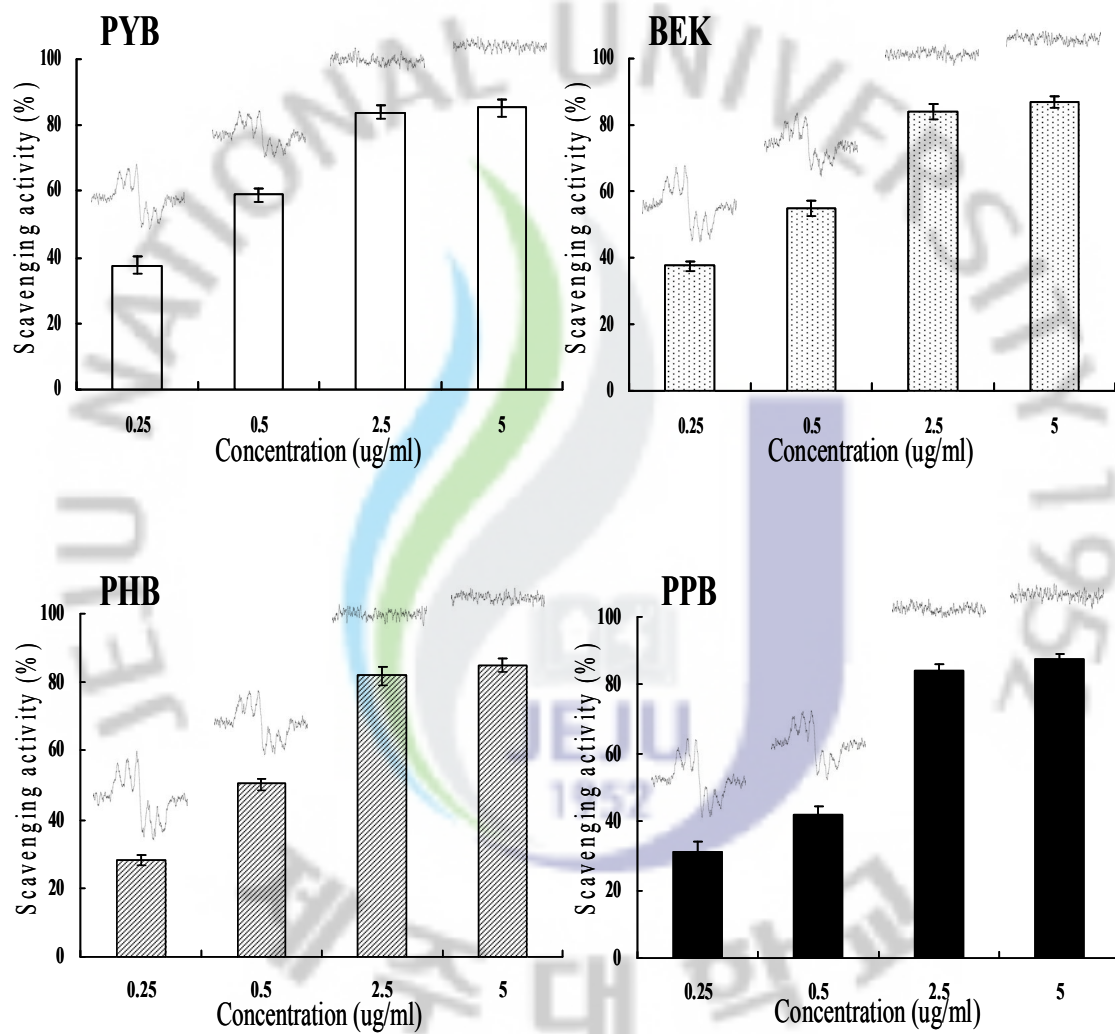


Fig. 1-16. DPPH radical scavenging activity of the active compounds isolated from *E. cava*. Experiments were performed in triplicate and the data are expressed as mean \pm SE.

Alkyl radical scavenging assay

The alkyl radical has been identified as a primary intermediate in many hydrocarbon reactions. These radicals can be readily detected via the ESR technique, which has proven to be extraordinarily useful in the characterization of solid surface and in the elucidation of active surface sites, as well as surface reactions. The scavenging activities of active compounds isolated from *E. cava* on alkyl radical are shown in Fig. 1-17. All compounds showed strong alkyl radical scavenging activity. Among four compounds, PYB showed the highest IC₅₀ value for Alkyl radical scavenging activity (IC₅₀=1.76 ug/ml) and the IC₅₀ value of BEK, PHB, and PPB were 1.92, 2.02, and 2.48 ug/ml, respectively, and the activity was dose-dependent. The decrease of ESR signal was observed with the dose increment of compounds (Fig. 1-17). Therefore, the active compounds isolated from *E. cava* would appear to be a potential alkyl radical scavenger.

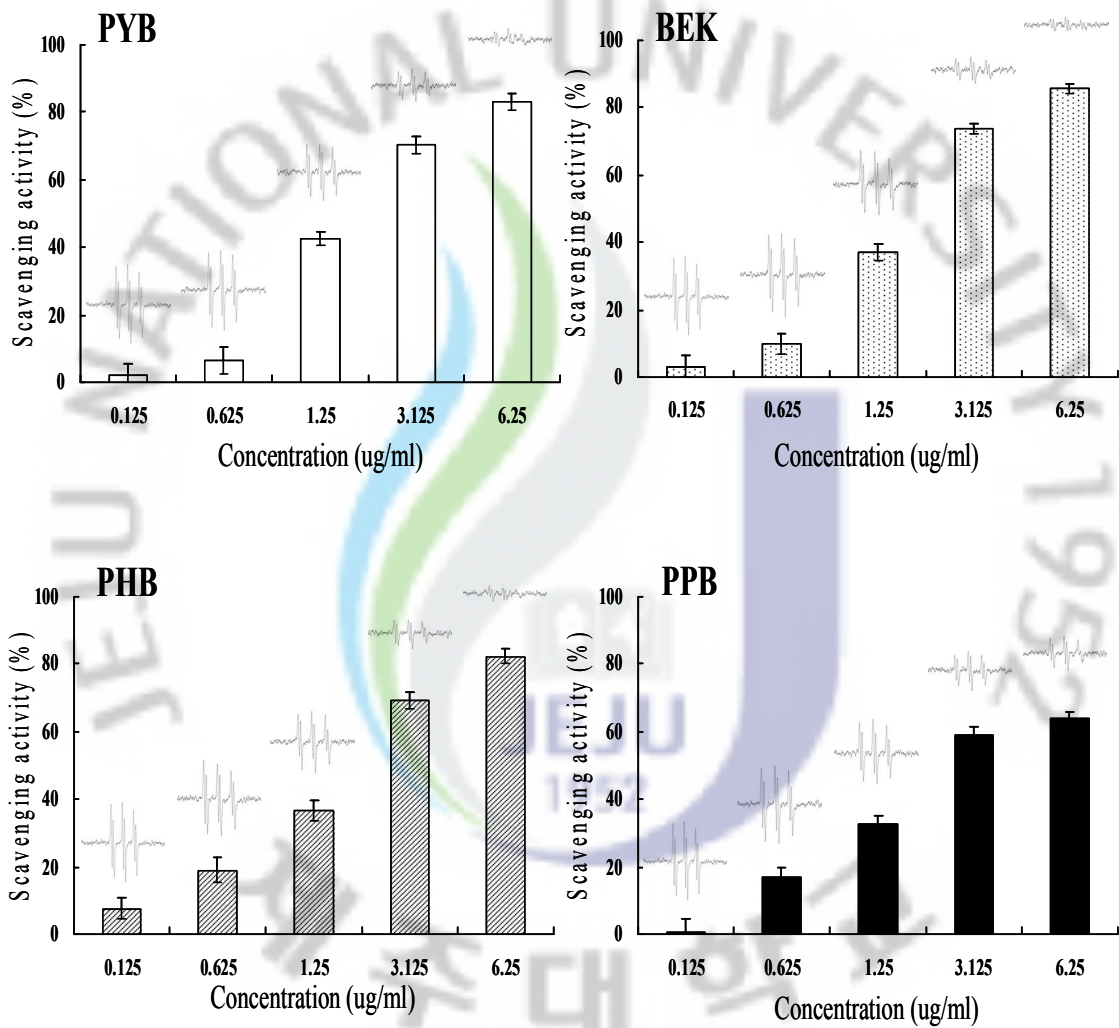


Fig. 1-17. Alkyl radical scavenging activity of the active compounds isolated from *E. cava*. Experiments were performed in triplicate and the data are expressed as mean \pm SE.

Hydroxyl radical scavenging assay

The HO· has an extremely short half-life and can be measured by using spin traps, such as DMPO. The spin trap and HO· form a stable DMPO– adduct, which can be easily measured by ESR. The Fenton reaction was applied as a source of HO radicals :



The hydroxyl radical scavenging activity of active compounds calculated by the height of the third peak of the spectrum which represents the relative amount of DMPO-OH adducts. After the addition of compounds, the decrease of the amount of DMPO-OH adduct was shown on the ESR spectrum (Fig. 1-18). The scavenging activities of active compounds isolated from *E. cava* on hydroxyl radical are shown in Fig. 1-18. All compounds showed strong hydroxyl radical scavenging activities. Among the four compounds, PYB showed the highest IC₅₀ value for hydroxyl radical scavenging activity (IC₅₀=39.54 ug/ml) and the IC₅₀ values of the compounds BEK, PHB, and PPB were 41.75, 73.68, and 61.30 ug/ml, respectively.

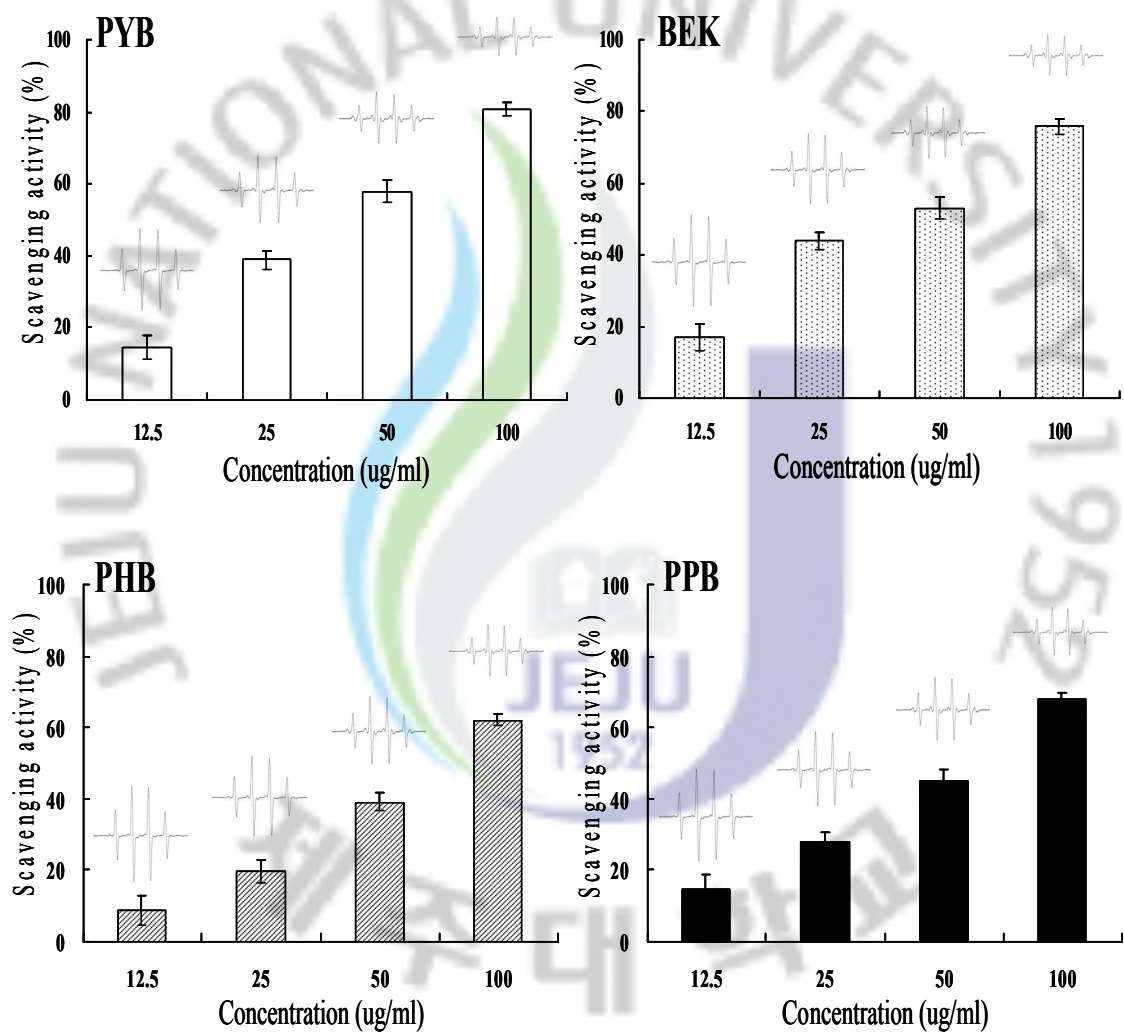


Fig. 1-18. Hydroxyl radical scavenging activity of the active compounds isolated from *E. cava*. Experiments were performed in triplicate and the data are expressed as mean \pm SE.

Superoxide radical scavenging assay

Superoxide radical is known to be very harmful to cellular components as a precursor of other reactive oxidative species, such as single oxygen and hydroxyl radicals. Superoxide radicals were generated by UV irradiation of a riboflavin/EDTA system and trapped as DMPO spin adduct was measured by ESR spectrometer (Fig. 1-19).

The superoxide radical scavenging activities of active compounds isolated from *E. cava* on superoxide radical are shown in Fig. 1-19. All compounds showed strong superoxide radical scavenging activities. Among the four compounds, PYB showed the highest IC₅₀ value for superoxide radical scavenging (IC₅₀=18.50 ug/ml) and the IC₅₀ values of BEK, PHBA, and PPB were 20.27, 55.71, and 106.22 ug/ml, respectively, and radical scavenging activity was dose-dependent.

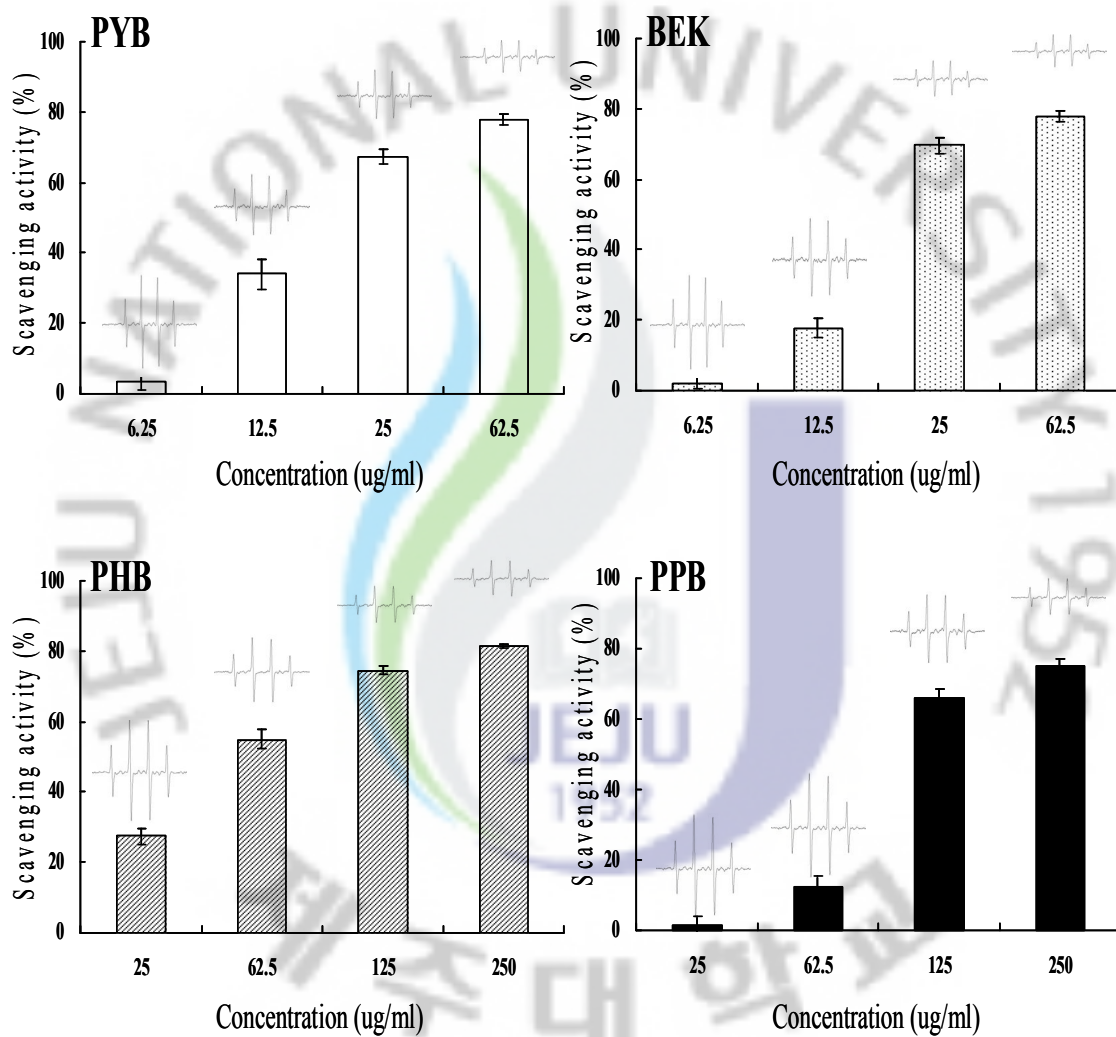


Fig. 1-19. Superoxide radical scavenging activity of the active compounds isolated from *E. cava*. Experiments were performed in triplicate and the data are expressed as mean \pm SE.

Intracellular reactive oxygen (ROS) species measurement

To determine whether compounds could prevent H₂O₂-induced ROS generation and the resulting oxidative stress, levels of ROS production in the cells were determined using the fluorescence probe DCF. In this study, we investigated the antioxidant effects of the isolated compounds after the administration of H₂O₂ in Vero cell lines. The intracellular ROS scavenging activity of the compounds was shown in Fig. 1-20. Among the four compounds, BEK showed the highest intracellular ROS scavenging activity (IC₅₀=2.01 ug/ml) and the compounds PYB, PHB, and PPB showed IC₅₀ value as 2.49, 2.40, and 3.54 ug/ml, respectively, and intracellular ROS scavenging activity of those compounds increased with increased concentrations, from 0.5 ug/ml to 5 ug/ml.

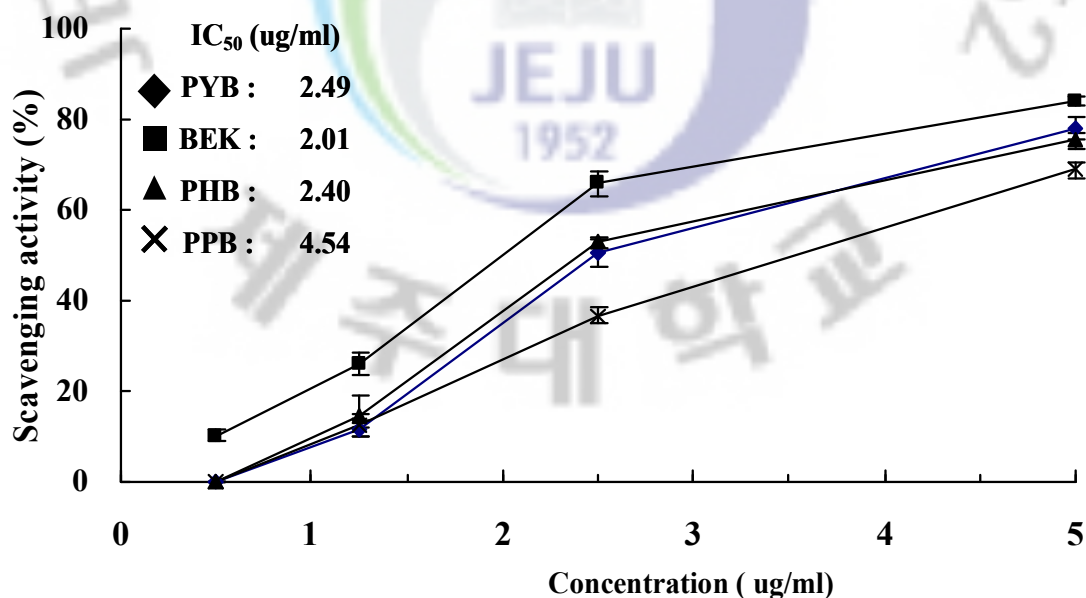


Fig. 1-20. Effect of the compounds isolated from *E. cava* on scavenging reactive oxygen species. The intracellular reactive oxygen species generated was detected by DCF-DA method. Experiments were performed in triplicate and the data are

expressed as mean \pm SE.

Protective effect against H₂O₂-induced cell damage

The protective effect of active compounds on cell damages were also confirmed by comet assay (Fig. 1-21, 23, 25, 27) photomicrographs of different DNA migration profiles, when treated with different concentrations of the isolated compounds are given in Fig. 1-22, 24, 26, 28. In the cells exposed to only H₂O₂, the DNA was completely damaged but the addition of compounds with H₂O₂ effectively suppressed DNA damage. As shown in results, remarkable scavenging effects were observed for active compounds (PYB, BEK, PHB, and PPB) where the compounds showed 40.6, 54.9, 53.6 and 50.6 % of the DNA damage inhibition activity even at the 25 ug/ml concentration. Among the four compounds, BEK showed the highest IC₅₀ value for DNA damage inhibition activity (IC₅₀=23.2 ug/ml) and the compounds PYB, PHB, and PPB showed IC₅₀ values 36.9, 24.1, and 24.7 ug/ml, respectively, and hydrogen peroxide scavenging activity of those compounds increased with increased concentrations from 12.5 ug/ml to 50 ug/ml (Fig. 1-22, 24, 26, 28).

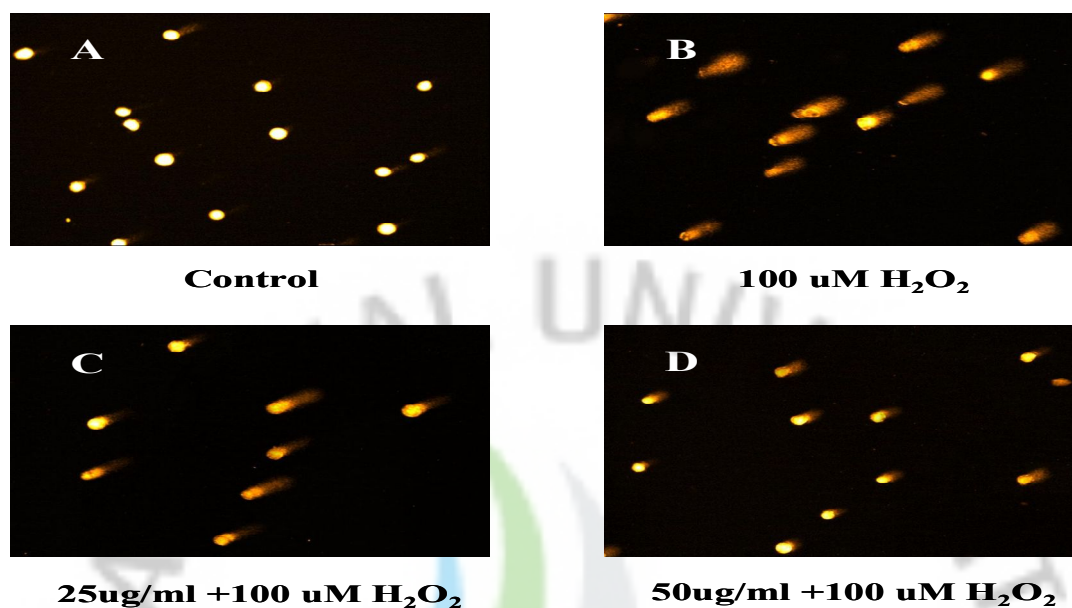


Fig. 1-21. Photomicrographs of DNA damage and migration observed under PYB isolated *E. cava*. A, control; B, 100uM H₂O₂; C, 25 ug/ml of compound + 100uM H₂O₂; D, 50 ug/ml of compound + 100uM H₂O₂.

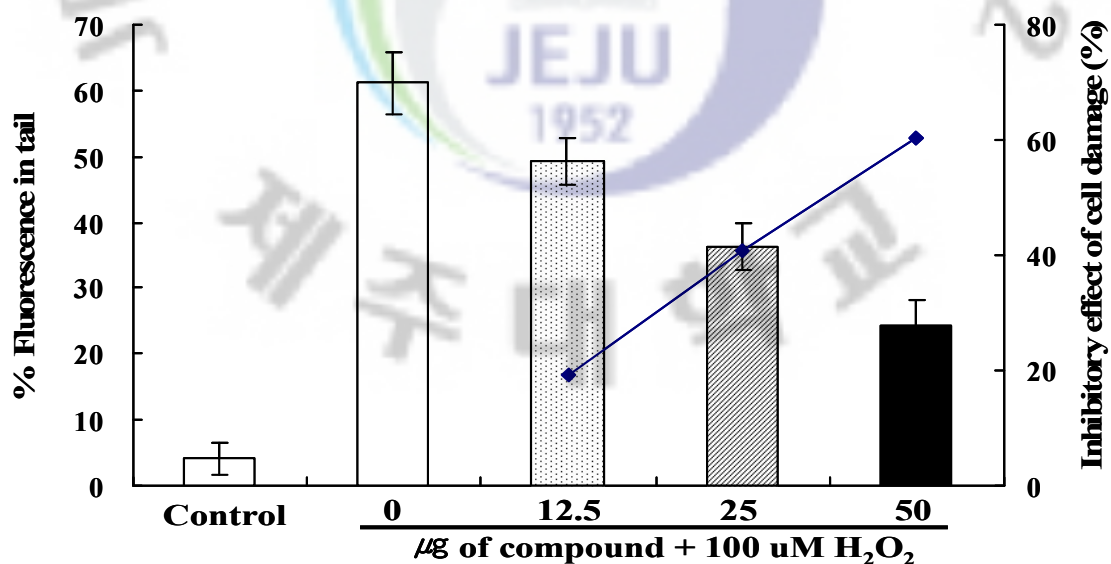


Fig. 1-22. Inhibitory effect of different concentrations of PYB isolated *E. cava* on H₂O₂ induced DNA damage. The damage cells on H₂O₂-treatment were determined by comet assay. □, % Fluorescence in tail; ◆, Inhibitory effect of cell damage.

Experiments were performed in triplicate and the data are expressed as mean \pm SE.

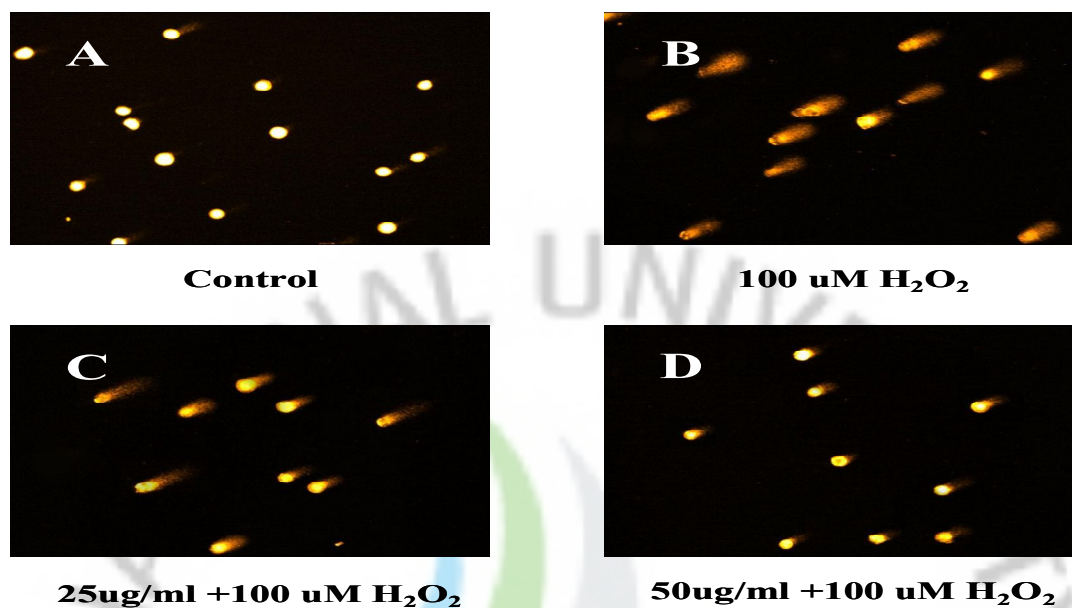


Fig. 1-23. Photomicrographs of DNA damage and migration observed under BEK isolated *E. cava*. A, control; B, 100uM H₂O₂ ; C, 25 ug/ml of compound + 100uM H₂O₂ ; D, 50 ug/ml of compound + 100uM H₂O₂.

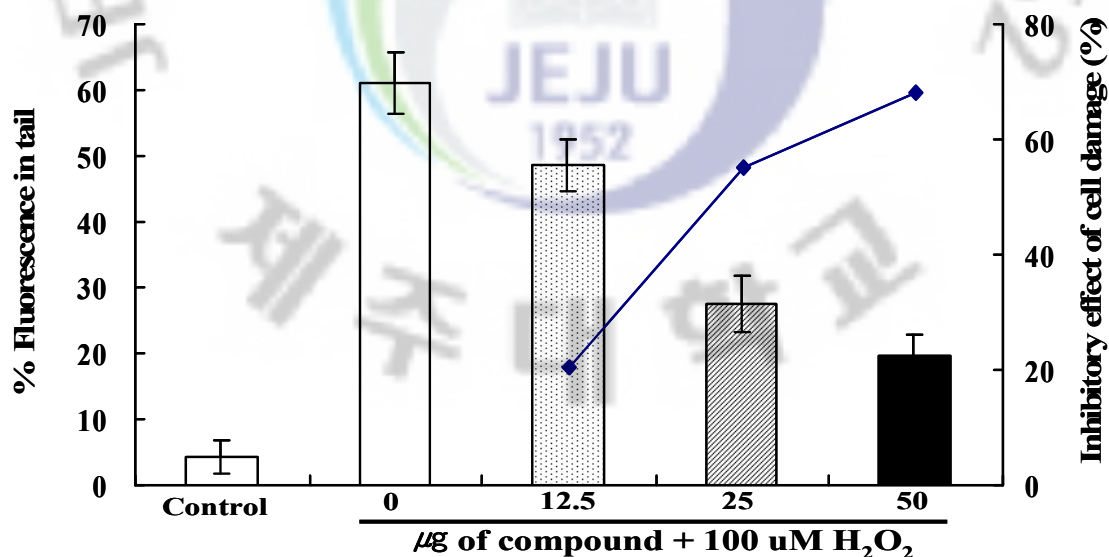


Fig. 1-24. Inhibitory effect of different concentrations of BEK isolated *E. cava* on H₂O₂ induced DNA damage. The damage cells on H₂O₂-treatment were determined by comet assay. \square , % Fluorescence in tail; \blacklozenge , Inhibitory effect of cell damage. Experiments were performed in triplicate and the data are expressed as mean

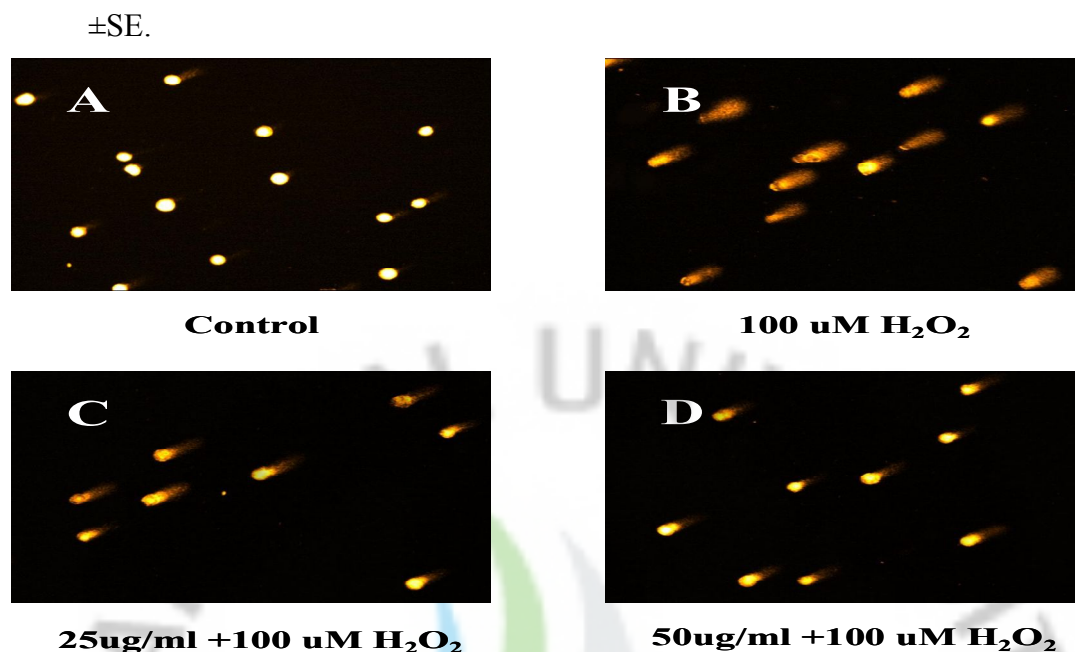


Fig. 1-25. Photomicrographs of DNA damage and migration observed under PHB isolated *E. cava*. A, control; B, 100uM H₂O₂ ; C, 25 ug/ml of compound + 100uM H₂O₂ ; D, 50 ug/ml of compound + 100uM H₂O₂.

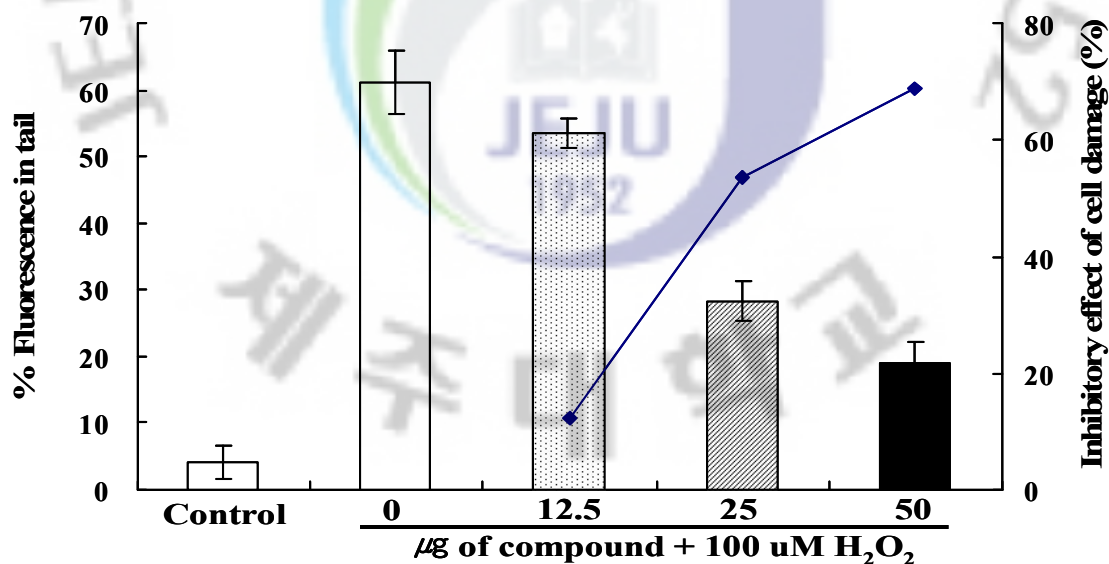


Fig. 1-26. Inhibitory effect of different concentrations of PHB isolated *E. cava* on H₂O₂ induced DNA damage. The damage cells on H₂O₂-treatment were determined by comet assay. □, % Fluorescence in tail; ◆, Inhibitory effect of cell damage. Experiments were performed in triplicate and the data are expressed as mean ±SE.

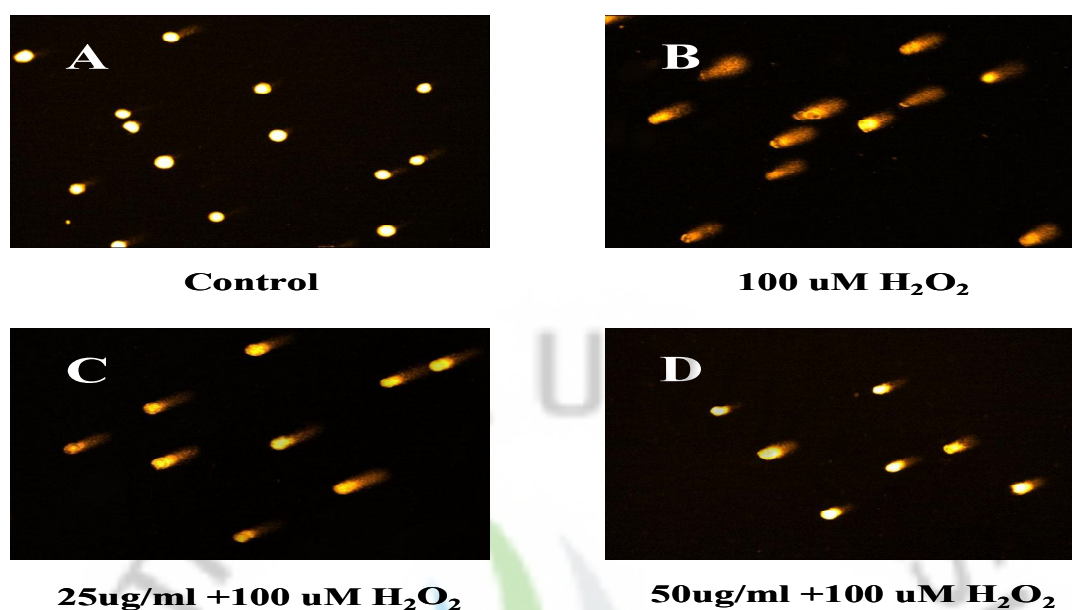


Fig. 1-27. Photomicrographs of DNA damage and migration observed under PPB isolated *E. cava*. A, control; B, 100uM H₂O₂ ; C, 25 ug/ml of compound + 100uM H₂O₂ ; D, 50 ug/ml of compound + 100uM H₂O₂.

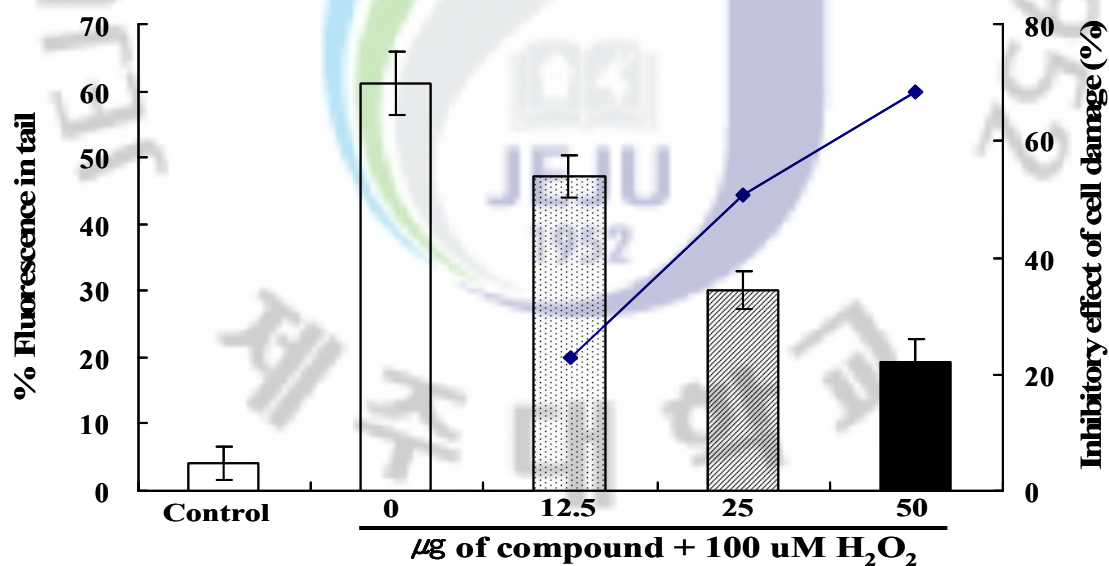


Fig. 1-28. Inhibitory effect of different concentrations of PPB isolated *E. cava* on H₂O₂ induced DNA damage. The damage cells on H₂O₂-treatment were determined by comet assay. □, % Fluorescence in tail; ◆, Inhibitory effect of cell damage. Experiments were performed in triplicate and the data are expressed as mean \pm SE.

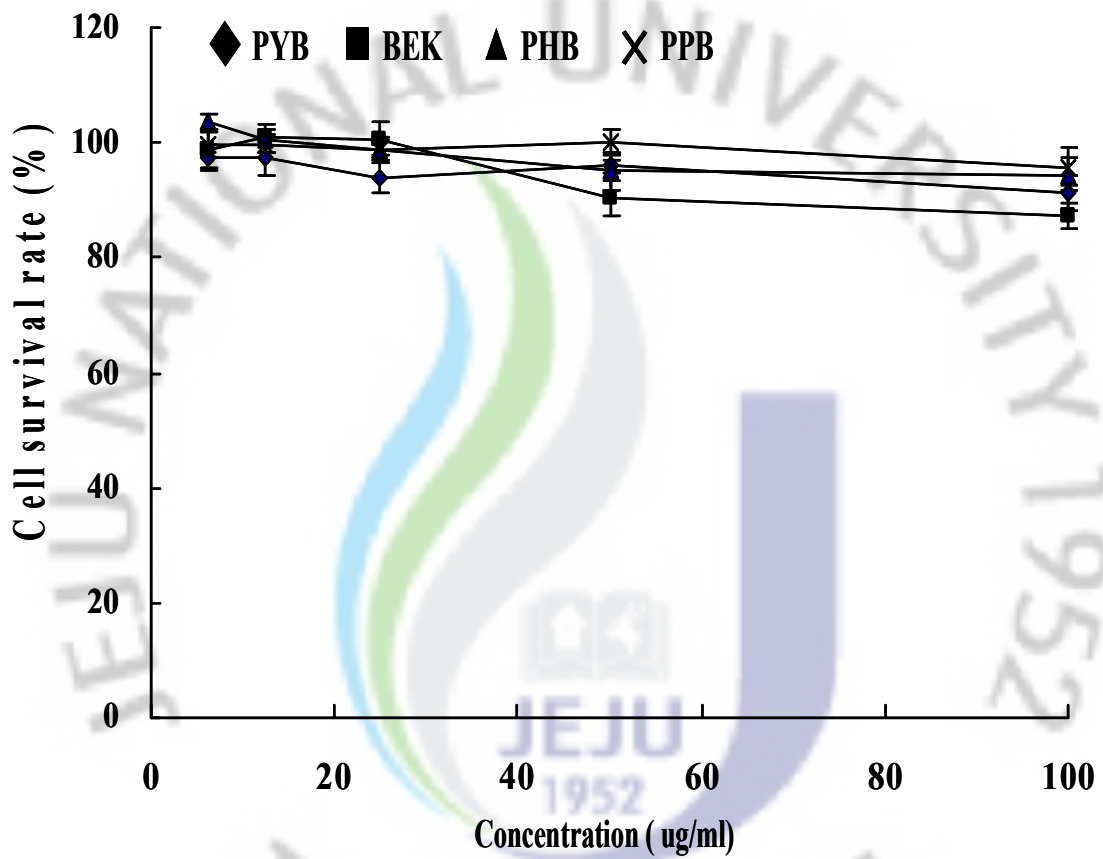


Fig. 1-29. Cytotoxic effects of the active compounds isolated from *E. cava*. The viability of Vero cell was determined by MTT assay. Experiments were performed in triplicate and the data are expressed as mean \pm SE.

4. DISCUSSION


80% methanol extracted active compounds were purified by celite column, silica column, sephadex LH-20 column, and RP-HPLC, and the purified compounds ((pyrogallol-6,6'-bieckol (PYB), 6,6'-bieckol (BEK), 2,7''-phloroglucinol-6,6'-bieckol (PHB), pyrogallol-phloroglucinol-6,6'-bieckol (PPB)) were confirmed high purity.

We examined the antioxidant activities of active compounds isolated from *E. cava* (PYB, BEK, PHB, and PPB as shown in Fig. 1-2) using Vero cells. DPPH radicals, alkyl radicals, hydroxyl radicals, superoxide radicals, and Intracellular reactive oxygen species (ROS) were evaluated in this study, oxidative DNA damage. It has been considered that antioxidants play a crucial role to reduce the oxidative stress in the living body. It was observed that PYB, BEK, PHB, and PPB reduced DPPH radicals effectively between the concentrations 0.25-5 ug/ml (Fig. 1-16); PYB, BEK, PHB, and PPB reduced alkyl radicals at concentrations with 0.625-6.25 ug/ml (Fig. 1-17); PYB, BEK, PHB, and PPB reduced hydroxyl radicals effectively between the concentrations 12.5-100 ug/ml (Fig. 1-18); PYB, BEK, PHB, and PPB reduced superoxide radicals effectively between the concentrations 6.25-62.5 ug/ml (Fig.1-19). These results showed that isolated compounds can be regarded as potent ROS scavengers. Secondly, the intracellular oxidative stress induced H₂O₂ were measured by DCFH-DA method. It was clear that isolated compounds PYB, BEK, PHB, and PPB showed strong ROS scavenging effect against H₂O₂-induced damage (Fig. 1-20). The sample didn't show any cytotoxic effect even at a high concentration on Vero cell (Fig. 1-29). Additionally, the cytoprotective effects of isolated compounds against H₂O₂-induced DNA damage in Vero cells were evaluated (Fig.1-21~28). The active compounds (PYB, BEK, PHB, and

PPB) inhibited H₂O₂-induced DNA damage effectively. When active compounds were added to the cell induced by H₂O₂, the significant inhibitory effects were observed. This result was consistent with the studies conducted by ESR spin trapping method.

In conclusion, our results revealed that the active compounds isolated from *E. cava* showed at different magnitudes of potency and protective effect against H₂O₂ induced damage in Vero cells. Thus, the results suggest that the active compounds (PYB, BEK, PHB, and PPB) isolated from *E. cava* could be used as a potential natural antioxidant agents in pharmaceutical and food industry.





Part II.
**Anti-inflammatory activity of
polysaccharide purified from AMG
extract of *E. cava* in LPS-stimulated
RAW 264.7 macrophages**

ABSTRACT

Ecklonia cava has reported anti-thrombotic, immunomodulatory and anti-inflammatory effects *in vitro* and *in vivo*. We evaluated the potential activity of the derivatives such as the sulfated polysaccharide from *E. cava* on anti-inflammatory activity in LPS-stimulated RAW 264.7 cell. In this study, *E. cava* was collected from Jeju Island of Korea and hydrolyzed by food grade and less expensive carbohydrases and proteases. We showed the AMG digest, which is the product hydrolyzed by AMG, has the highest inhibitory effects on NO production in LPS-stimulated RAW 264.7 cells. To identify the active compounds from the AMG digest, we performed the molecular membrane system, the ethanol separation, the anion exchange and gel permeation chromatography, and the 50 kDa over fraction, the crude polysaccharide (CPS) and the purified polysaccharide (PPA) were obtained. The AMG digests' derivatives (50 kDa over fraction, CPS and PPA) significantly inhibited the NO production and PPA showed the highest inhibitory activity on NO production. Also, PPA decreased the prostaglandin-E₂ (PGE₂) production and suppressed the inducible nitric oxide synthase (iNOS) and cyclooxygenase-2 (COX-2) expression in the LPS-stimulated Raw 264.7 cells. Thus, the PPA inhibited NO and PGE₂ production through the inhibition of iNOS and COX-2 expression in LPS-stimulated RAW 264.7. These results suggest that the anti-inflammatory activity of PPA may be due to modulation of anti-inflammatory agent.

1. INTRODUCTION

Inflammation is the process by which the human body attempts to counteract potential injurious agents such as invading bacteria, viruses, and other pathogens (Henderson et al., 1996; Ulevitch and Tobias, 1995; Hersh et al., 1998). Although it is an essential process in the living organisms, inflammation can also produce harmful effect to the host through the multiple levels of biochemical, pharmacological, and molecular controls involving a diverse array of cell types and some soluble mediators including cytokines (Nicod, 1993; Rouveix, 1997; Boraschi et al., 1998; Dinarello, 2000; Turcanu et al., 2001). When the pro-inflammatory cytokines like IL-1 β , IL-6, and TNF- α are administered to humans, they produce fever, inflammation, tissue destruction, and in some cases, shock and death (Dinarello, 2000).

In these mediators, NO is generated enzymatically by nitric oxide synthases (NOS) and is formed by iNOS in macrophages and in other cells that plays a role in the inflammatory response. Large amounts of NO can stimulate many proteins and enzymes crucial to inflammatory reactions, such as the NF- κ B and MAPKs pathways (Nijkamp and Parnham, 2005). Many studies have reported that MAPKs mediate the activation of transcriptional factor NF- κ B (DeFranco et al., 1995; Aga et al., 2004) and, subsequently, regulate COX-2 expression (Mestre et al., 2001) as well as iNOS-NO expression (Chan and Riches, 2001). Furthermore, iNOS expression and NO production, both stimulated by LPS, have been proved to contribute to septic shock (Jacobs et al., 2001). Prostaglandin E₂, one of the prostaglandins, is produced by the cyclooxygenase pathway. Prostaglandins regulate vascular permeability, platelet aggregation and thrombus formation in the development of inflammation. Inhibition of COX-2 activity

can reduce the deleterious consequences of sepsis (Knofelr et al., 2001). All of these cytokines can be the targets in the treatment of inflammatory diseases, and a proper understanding of the inflammatory basis is helpful to understand atherosclerosis, cancer, ischemic heart disease, and other maladies. NO has been identified as an important molecule involved in regulating biological activities in the vascular, neural, and immune systems (Moncada et al., 1992). NO produced by activated macrophages has been shown to mediate host defense functions such as antimicrobial and anti-tumor activities, but its excess production causes tissue damage associated with acute and chronic inflammation (MacMicking et al., 1997).

Athukorala et al. (2006), isolated a highly sulfated polysaccharide from an enzymatic digest of *E. cava*. The highly sulfated active fraction was mainly composed of fucose and a small of galactose. The polysaccharide showed high anticoagulant and anticancer activity.

In this study, we investigated the anti-inflammatory effect of purified polysaccharide on LPS-stimulated macrophage RAW264.7 cells by NO, iNOS, COX-2 and PGE₂ assays.

2. MATERIAL AND METHOD

2.1. Plant material and extraction

E. cava was collected along Jeju Island coast of Korea during February and May 2007. Salt, sand and epiphytes were removed using tap water. Then, seaweed samples were rinsed carefully with fresh water and freeze-dried. Dried alga sample was ground (MFC SI mill, Janke and Kunkel Ika-Wreck, Staufen, Germany) and sifted through a 50-mesh standard testing sieve. The preparation of enzymatic digests was followed by previously reported method (Heo et al., 2003). Fifty gram of alga sample was homogenized with water (2 L), and mixed with 500 μl of enzymes. Each reactant was adjusted to be within the optimum pH and temperature range of the respective enzyme and enzymatic reactions were performed for 24 hr. Following digestion, the digest was boiled for 10 min at 100 °C to inactivate the enzymes. Then, samples were clarified by centrifugation (3000 rpm, for 20 min at 4 °C) to remove the residue. This extracts were adjusted to pH 7.0 hereafter and designated to as enzymatic extract. The sample was kept in -20 °C for further experiments.

2.2. Molecular weight fractionation of AMG extract

AMG digest was passed through micro-filtration membrane (0.1 μm and 50 kDa) using Lab scale TFF system (PHILOS) to obtain different molecular weight fractions. Then, all the fractions (< 0.1 μm , >50 kDa, <50 kDa) were separately evaluated for anti-inflammatory activity.

2.3. Crude polysaccharide separation

The > 50 kDa fraction was (750 ml) mixed well with 1.5 L of 99.5 % ethanol. Then, the mixture was allowed to stand for 30 min at room temperature and crude polysaccharide fractions were collected by centrifugation at 10,000g for 20 min at 4 °C (Kuda, Taniguchi, Nishizawa, & Araki, 2002; Matsubara, Hori, & Miyazawa, 2000).

2.4. Anion-exchange chromatography

The crude polysaccharide from *E. cava* (5 g) obtained by using the procedures described above was applied to a DEAE-cellulose column (17 x 2.5 cm) equilibrated in 50 mM sodium acetate (pH 5.0) and washed with the same buffer containing 0.2 M NaCl. Elution was carried out at a flow rate 15 ml/h with a liner gradient of 0.2-1.2 M NaCl containing 50 mM sodium acetate (pH 5.0). Fractions of 5 ml were collected and measured for polysaccharide by phenol-H₂SO₄, carbazole reactions and by metachromatic property (Chaplin & Kenndy, 1994). Fractions showing anti-inflammatory activities were collected, dialyzed against distilled water, and concentrated to 5 ml by rotary evaporator under reduced pressure bellow 40 °C. The partially purified concentrated polysaccharide fraction was re-chromatographed on new DEAE-cellulose column (10 x 1.7 cm), under same experimental condition. The active fractions were pooled, dialyzed and freeze dried for gel filtration chromatography.

2.5. Gel filtration chromatography

Purified sample (10 mg/ml in water) was applied to a Sepharose 4B column (72 x 2 cm) equilibrated and eluted with water at room temperature at a flow rate of 1 ml/min. Fractions (2 ml) were collected and assayed for metachromatic property at 525 nm and

for total polysaccharide contents.

2.6. Determination of the Molecular Mass of the purified polysaccharide

In order to determine the molecular mass of the sample, the freeze-dried sample was introduced into PL-Aquaz OH 40 column and eluted with deionized water at 0.8 ml/min flow rate. Dextran standards (48.6, 148, 273, 410, 830, and 2,000 kDa) were also introduced into the column under the same experimental condition for comparison purposes. The retention time was plotted against average molecular mass of the dextrans, and there by the molecular mass of the sample was calculated.

2.7. Neutral sugar analysis

The *E. cava* fractions were hydrolyzed in a sealed glass tube with 4 M of trifluoroacetic acid for 4 hr at 100 °C to analyze neutral sugars. In order to analyze the amino-sugars the samples were digested using 6 N of HCl for 4 hr. Then, *E. cava* fractions were separately applied to CarboPac PA1 (4.5 x 250 mm, Dionex, Sunnyvale, CA, USA) with CarboPac PA1 cartridge (4.5 x 50 mm) column to analyze neutral and amino sugar respectively. The column was eluted using 16 mM of NaOH at 1.0 ml/min flow rate. Each sugar of the sample was detected by using ED50 Dionex electrochemical detector and data were analyzed by Peak Net on-line software.

2.8. Sulfate content analysis

After acid hydrolysis of the purified polysaccharide, the sulfate content was measured by the BaCl₂/gelation method (Saito, Yamagata, & Suzuki, 1968).

2.9. Cell culture

Murine macrophage cell line RAW264.7 was obtained from the KCLB (Korean Cell Line Bank). The cells were maintained at 37°C in humidified atmosphere of 5% CO₂ in DMEM medium supplemented with 10% fetal bovine serum and penicillin / streptomycin (100 U/mL and 100 µg/mL, respectively; GIBCO Inc, NY, U.S.A). Exponential phase cells were used throughout the experiments.

2.10. Nitrite assay

The cells (1 X 10⁵ cell/ml) were pretreated with various concentrations of purified compounds (6.25, 12.5, 25, 50 µg/ml) for 2 hr and then incubated for 24 hr with LPS (1µg/ml). After incubation, the nitrite concentrations of supernatants (100 µl/well) were measured by adding 100 µl of Griess reagent (1% sulfanilamide in 2.5% phosphoric acid and 0.1% naphthylendiamine dihydrochloride in water). The optical density at 540 nm was measured using an ELISA microplate reader (Amersham Pharmacia Biotech, UK, U.S.A.). The nitrite concentration was calculated by comparison with the absorbance at 540 nm of standard solutions of sodium nitrite prepared in culture medium.

2.11. Western blot analysis of COX-2 and iNOS in RAW 264.7 cells

Murine macrophage cell line RAW264.7 were pre-incubated for 16 hr, and then stimulated by LPS (1µg/ml) in the presence or absence of purified compounds for 24 hr. The cells were harvested, washed twice with ice-cold phosphate-buffered saline (PBS), and the cell lysates were prepared with lysis buffer (50 mM/L Tris-HCl (pH 7.4), 150 mM/l NaCl, 1% Triton X-100, 0.1% SDS and 1 mM/L EDTA) for 20 min on ice.

Cell lysates were centrifuged at 14,000 g for 20 min at 4 °C. And then protein contents in the supernatant were measured using BCATM protein assay kit. The lysate containing 20 µg of protein were subjected to electrophoresis on 7.5% sodium dodecyl sulfate-polyacrylamide gel, and the gel was transferred onto a nitrocellulose membrane (Bio-Rad, Hercules, CA). The membranes were blocked with 5% non-fat dry milk in TBS buffer containing 0.2% Tween 20 (TBST) for 90 min at room temperature. Then the membrane was incubated with specific primary rabbit polyclonal anti-rabbit iNOS Ab (1:2,000, Calbiochem, U.S.A), or mouse monoclonal anti-mouse COX-2 Ab (1:5,000, BD Biosciences, U.S.A) at 4 °C for overnight. Membranes were washed with TTBS and incubated with goat anti-mouse or anti-rabbit IgG HRP conjugated secondary antibody (1:5000 dilution) in TBST that contained 2% non-fat dry milk for 90 min at room temperature. After three times washing with TBST for 10 min. Signals were developed using an ECL western blotting detection kit and exposed to X-ray films.

2.12. PGE₂ enzyme-linked immunosorbent assay (ELISA)

PGE₂ levels were analyzed using the prostaglandin E₂ Biotrack ELISA system (Amersham Biosciences, Piscataway, NJ) according to the manufacture's instructions. RAW264.7 cells (1 x 10⁵ cells/well) were pretreated with PPA (25, 50, 100 and 200 µg/ml) for 2 hr and then incubated with LPS (1 ug/ml) for 24 hr. PGE₂ concentrations of supernatants were with a PGE₂ ELISA assay kit (Alexis, USA).

3. RESULTS

3-1. Isolation and purification of active compounds from *Ecklonia cava* for anti-inflammation in RAW264.7 cell

E. cava was enzymatically extracted by several carbohydrases (Viscozyme, Celluclast, AMG, Termamyl, and Ultraflo) and proteases (Kojizyme, Alcalase, Protamex, Flavourzyme, and Neutase) to evaluate its anti-inflammatory effects. All the enzymatic extracts of *E. cava* showed strong anti-inflammatory activities and extract yield compared with those of other enzymatic extracts (Fig. 2-1). Of the tested extracts, the AMG digest of *E. cava* showed an outstanding anti-inflammatory activity on NO assay. However, the AMG extract showed pronounced NO assay and was therefore selected for further purification purposes. To identify the active compounds of the AMG extract, 50 kDa over fraction of the AMG extract was separated by molecular membrane system (PHILOS). And then, crude polysaccharide fraction of the 50 kDa fraction was separated by the ethanol precipitation technique. The freeze-dried crude polysaccharide sample was introduced to a DEAE-cellulose column with NaCl gradient to separate the anti-inflammation fraction. After being evaporated under a rotary evaporator, the dialyzed sample was further purified by gel-filtration chromatography on Sepharose 4B (Fig.2-2).

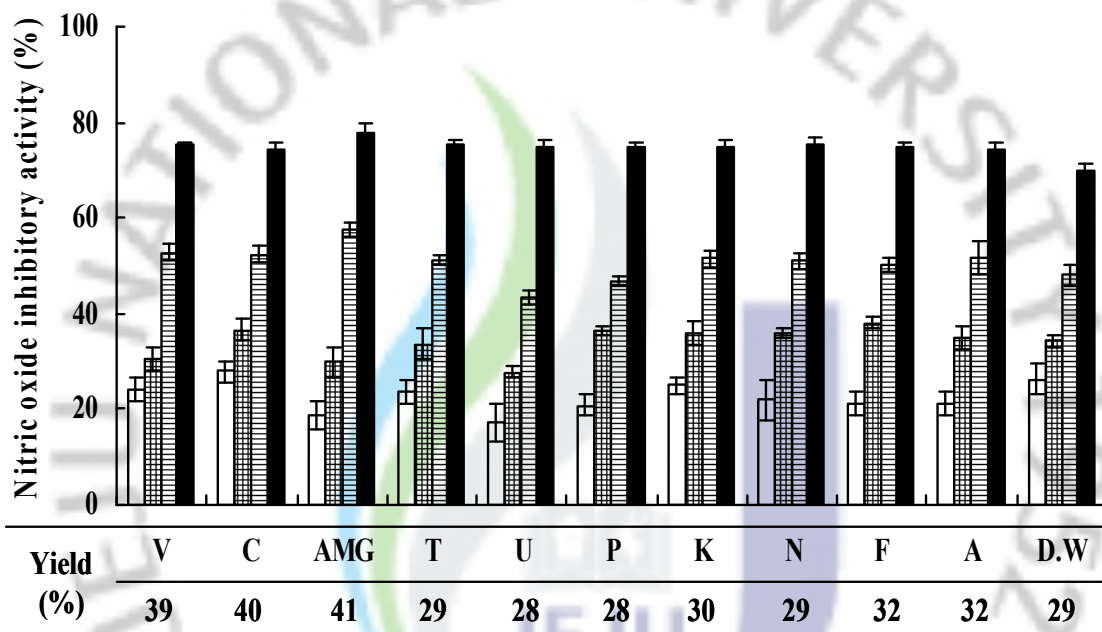


Fig. 2-1. Effects of enzymatic extract of *E. cava* on the inhibition activity of LPS-induced NO production in RAW264.7 cells. □, 25 ug/ml; ▤, 50 ug/ml; ▥, 100 ug/ml; ■, 200 ug/ml. V; Viscozyme extract, C; Celluclast extract, AMG; AMG extract, T; Termamyl extract, U; Ultraflo extract, P; Protamex extract, K; Kojizyme extract, N; Neutralse extract, F; Flavourzyme extract, A; Alcalase extract, D.W; Distilled water extract. Yield of enzymatic extracts of *E. cava* (%). Experiments were performed in triplicate and the data are expressed as mean \pm SE.

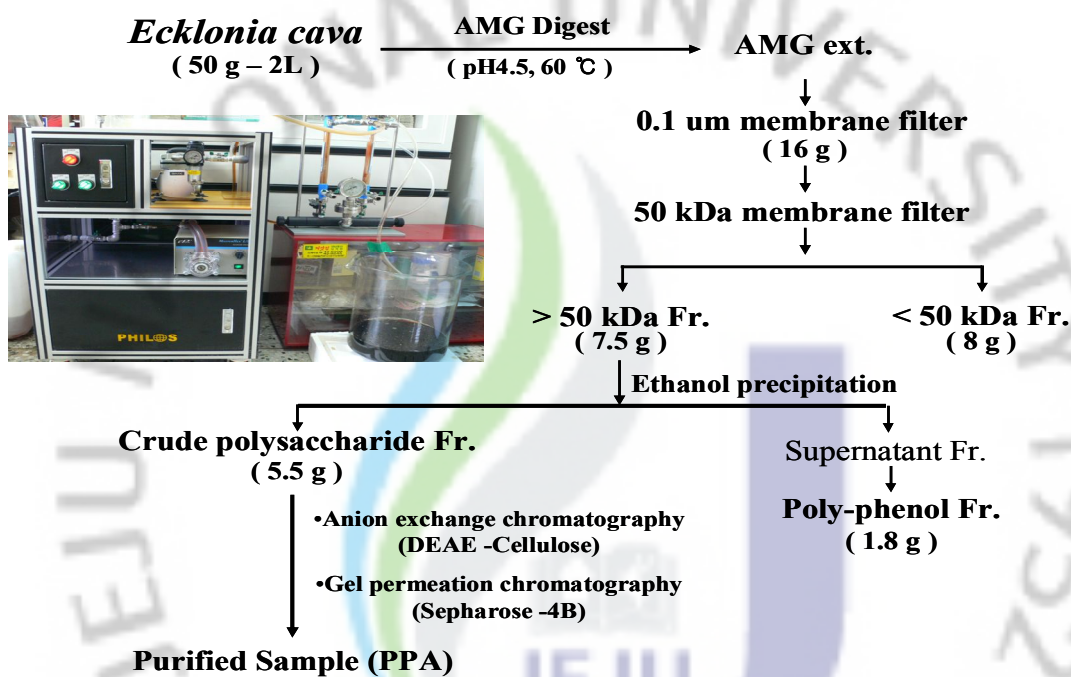


Fig. 2-2. Isolation and purification scheme of polysaccharide from AMG extract of *E. cava*.

3.2. Monosugar composition & sulfate contents analysis

The sugar composition of the active compound was investigated by Bio-LC and compared with the absorption spectra of standard sugars. Proximate monosugar composition of polysaccharide isolated from *E. cava* separated by molecular weight membrane, ethanol precipitation, and column-chromatography were shown in Table 2-1 and Fig. 2-3. According to the results, all fractions contains high amount of fucose (~48%, 65%, 69% and 82%) and less amount of galactose (~15%, 17%, 14% and 11%), respectively (Fig. 2-3). The separated fractions of polysaccharide towards fucose contents in increasing order, AMG ext, 50 kDa over Fr, CPS Fr, and PPA. Moreover all fractions contain minor amount of other sugars. The total sulfate content of the tested fractions were 0.41, 0.52, 0.71 and 0.92 (sulfate/total sugar), respectively (Table 2-1).

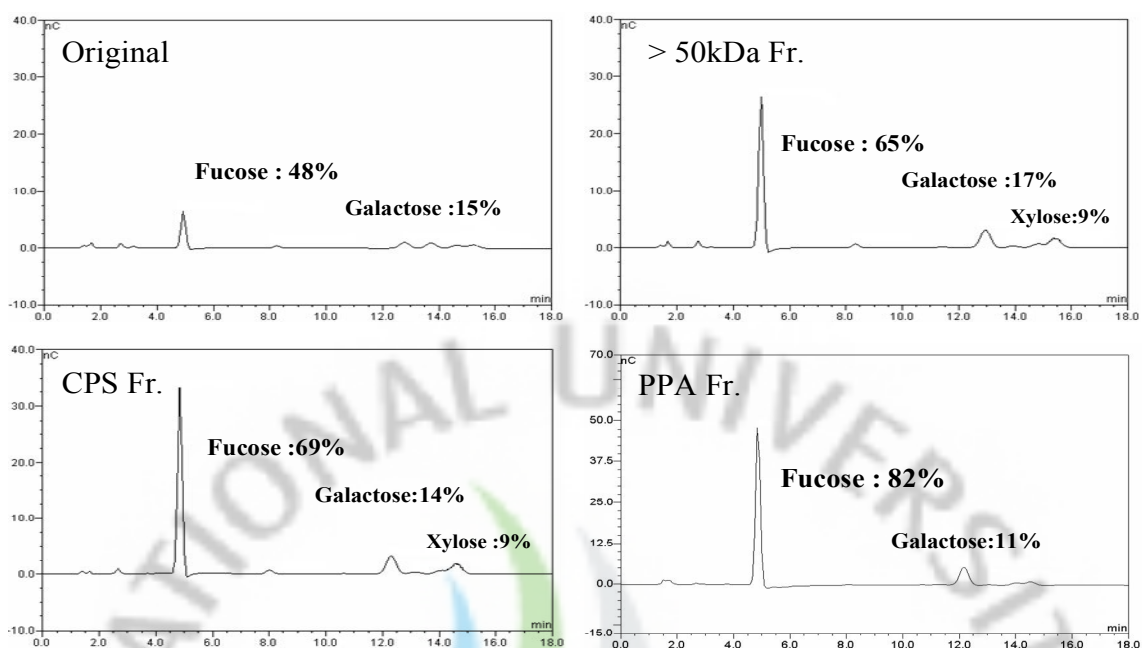


Fig.2-3. The Bio-LC chromatogram for the monosugar composition of the original, >50 kDa Fr, CPS, PPA of AMG extract from *E. cava*.

Table 2-1. Proximate monosugar composition of sulfated polysaccharide fraction isolated from AMG extract of *E. cava* separated by molecular weight membrane, ethanol precipitation, and column-chromatography

Sugar (%)	AMG ext	>50kDa Fr.	^b CPS Fr.	^c PPA
Fucose	48.17	65.13	69.55	82.11
Rhamnose	4.61	2.32	1.95	0.28
Galactose	15.28	17.32	14.95	12.21
Glucose	14.05	1.74	1.53	0.23
Mannose	8.53	4.01	2.69	2.07
Xylose	9.37	9.48	9.34	2.17
^a Sulfate/total sugar	0.41	0.52	0.71	0.92

^a The mean degree of substitution of sulfate ester per total sugar.

^b Crude polysaccharide, ^c Purified polysaccharide from AMG extract of *E. cava*.

3.3. Determination of the Molecular Mass of the purified polysaccharide

To investigate the exact molecular weight, the PPA was applied on HPLC gel filtration chromatography and the retention time of the PPA was plotted with known dextran standards. The molecular weight of the PPA was about 1381 kDa (Fig. 2-4).

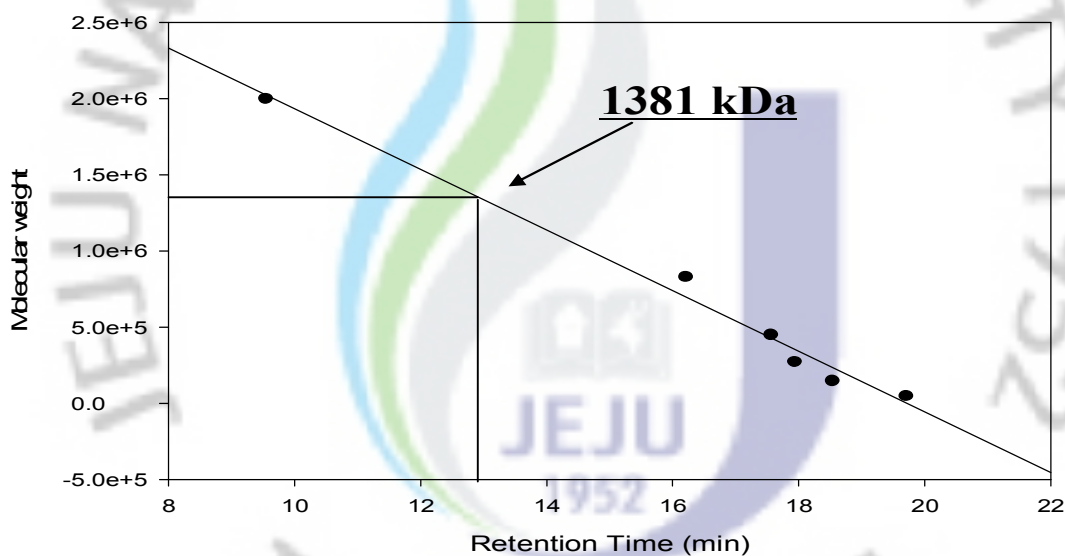


Fig. 2-4. Calibration curve of dextran standards for the determination of the average molecular weight of the *E. cava* sample. The retention time is plotted against the molecular weight of the dextrans.

3.4. Inhibition of NO production by separated polysaccharide fractions.

Stimulation of cells with LPS resulted in a significant enhancement of the nitrite concentration in conditioned medium compared with that of LPS non-stimulated blank cells (data not shown). This indicated increased production of NO and release of its stable product, NO_2^- , into the culture medium. However, cells pretreated with separated polysaccharide showed a dose-dependent reduction in the production of NO following stimulation with LPS. The separated fractions of polysaccharide towards inhibited NO production increased in the order of 50 kDa over fraction, CPS, and PPA, respectively (Fig. 2-5, 6). Moreover, even at the lowest tested concentration (3.125 ug/ml) of PPA, a significant reduction in the level of NO was observed. At 50 ug/ml of PPA, the level of NO production was similar to that of non-stimulated cells (Fig. 2.7).

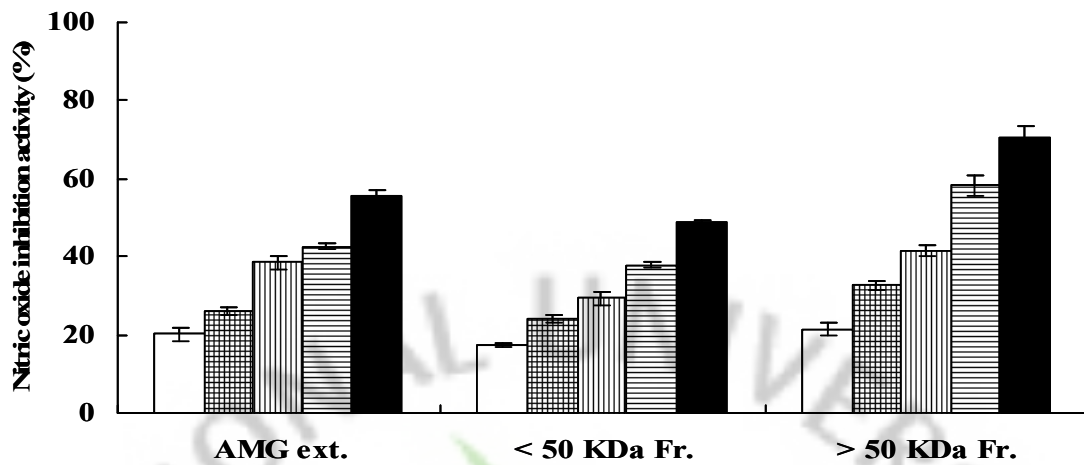


Fig. 2-5. Inhibitory effects of molecular weight fractions on LPS-induced NO (nitric oxide) production in RAW264.7 cells. □, 6.25 ug/ml; ▤, 12.5 ug/ml; ▥, 25 ug/ml; ▦, 50 ug/ml; ■, 100 ug/ml. Experiments were performed in triplicate and the data are expressed as mean ±SE.

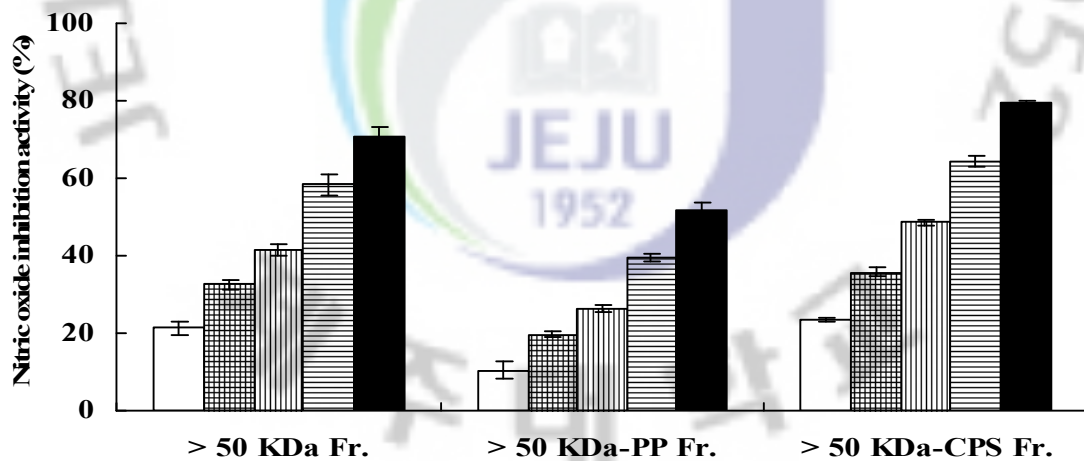


Fig. 2-6. Inhibitory effects of separated fractions (CPS) on LPS-induced NO production in RAW264.7 cells. □, 6.25 ug/ml; ▤, 12.5 ug/ml; ▥, 25 ug/ml; ▦, 50 ug/ml; ■, 100 ug/ml. Experiments were performed in triplicate and the data are expressed as mean ±SE.

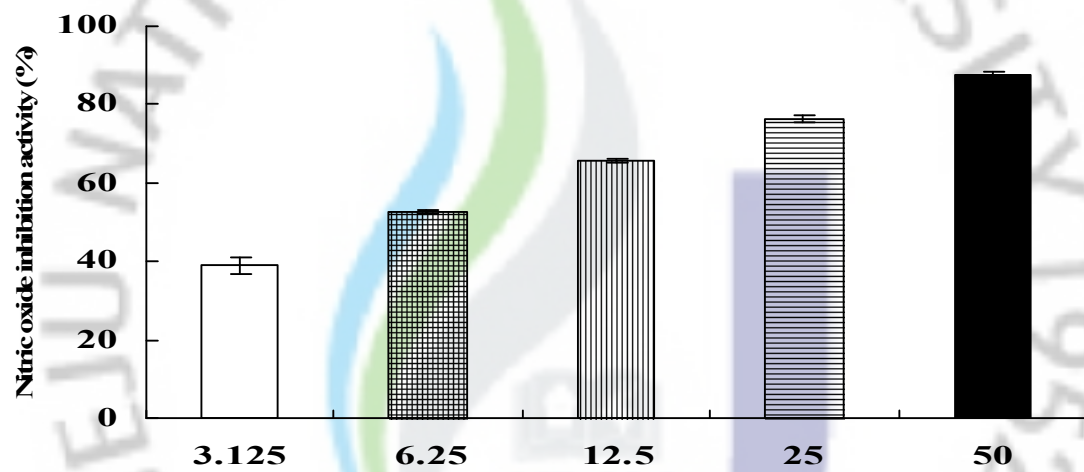


Fig. 2-7. Inhibitory effects of PPA on LPS-induced NO production in RAW264.7 cells.

□, 3.125 ug/ml; ▤, 6.25 ug/ml; ▥, 12.5 ug/ml; ▦, 25 ug/ml; ■, 50 ug/ml.

Experiments were performed in triplicate and the data are expressed as mean \pm SE.

3.5. Inhibition of iNOS expression and NO production by PPA

Inducible NO synthase (iNOS) is one of the major inflammatory mediator that contribute to the pathogenesis of cancer and inflammation. In response to LPS, the iNOS of macrophages is induced and sequentially leads to NO overproduction, which may play an important role in the pathogenesis of various inflammatory diseases. Our results showed that PPA significantly inhibited the NO production and iNOS expression in LPS-stimulated RAW264.7 macrophages, which may partly explain its anti-inflammatory effect. The PPA significantly inhibited this increase in NO production in a concentration-dependent manner, with 50 ug/ml PPA completely blocking the LPS-inducible NO production. It is unclear if the inhibition of NO formation by PPA is the result of the inhibition of iNOS gene expression. Therefore, the inhibitory effects of the different PPA concentration on iNOS protein expression induced by LPS (1 ug/ml) were assessed. As shown in Fig. 2-8, PPA concentration-dependently inhibited iNOS protein expression at 25~200 ug/ml.

These results showed that PPA suppresses the de novo synthesis of iNOS in LPS-stimulated macrophages.

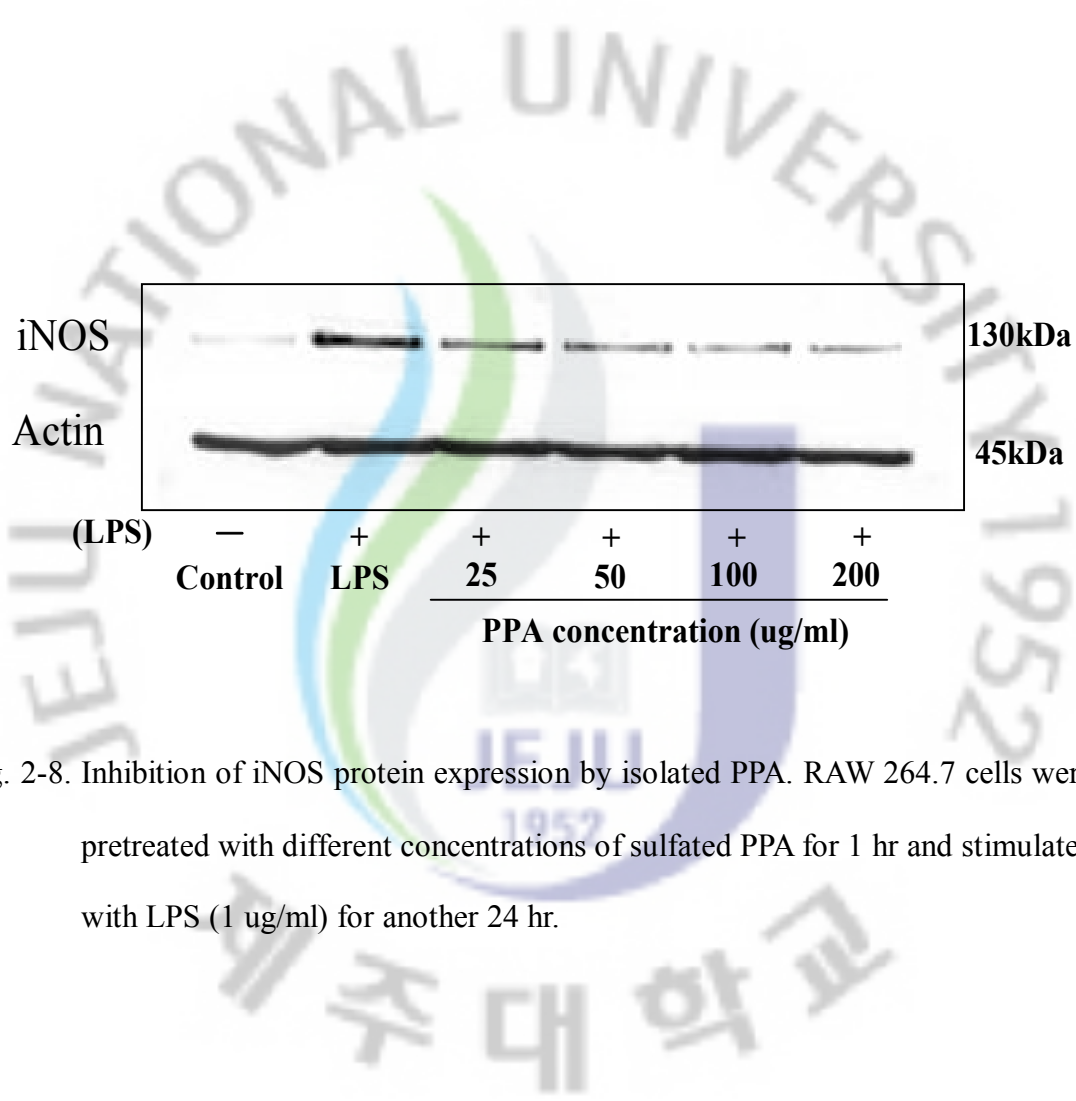


Fig. 2-8. Inhibition of iNOS protein expression by isolated PPA. RAW 264.7 cells were pretreated with different concentrations of sulfated PPA for 1 hr and stimulated with LPS (1 ug/ml) for another 24 hr.

3.6. Inhibition of PPA on COX-2 protein expression in RAW 264.7 cells

In order to confirm that the dose-dependent NO decrease is due to its influence on iNOS, the inhibitory effect of PPA on iNOS was measured by Western blot analysis. In addition, the inhibitory activity of PPA on COX-2 was also confirmed by means of western blot analysis. The COX-2 protein was induced upon LPS stimulation for 24 hr. As shown in Fig. 2-9, clear dose-dependent reductions of COX-2 is regulated by PPA in LPS-stimulated RAW 264.7 cells.

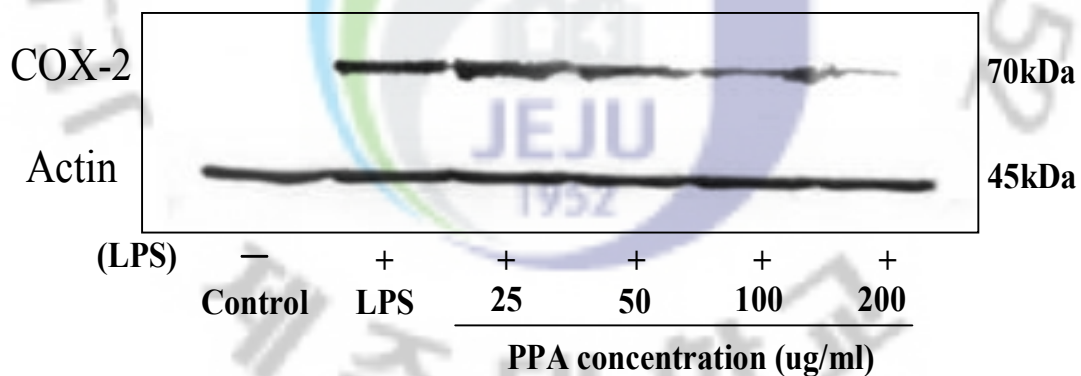


Fig. 2-9. Inhibition of COX-2 protein expression by isolated PPA. RAW 264.7 cells were pretreated with different concentrations of isolated PPA for 1hr and stimulated with LPS (1 ug/ml) for another 24 hr.

3.7. Inhibition of PPA on PGE₂ production in RAW 264.7 cells

To determine if the stimulatory effect of resin monomers on COX-2 protein expression were related to modulation of PGE₂ release, its production levels were examined by PGE₂ immunoassay. RAW 264.7 macrophages was treated with PPA (25, 50 100, and 200 ug/ml) for 24 hr, and the concentration of PGE₂ was estimated in cultured supernatants. Results demonstrated that upon the treatment with PPA, macrophages produced significantly lower PGE₂ in a dose-dependently when compared with the values obtained from LPS-treated cultures. The PPA significantly inhibited PGE₂ production in a concentration-dependent manner with 200 ug/ml PPA strongly blocking the LPS-inducible PGE₂ production. In order to determine the mechanism by which PPA reduced LPS-induced PGE₂ production, we studied the ability of PPA to influence LPS-induced expression of COX-2. The addition of LPS resulted in a clearly defined increase in COX-2 expression that was markedly attenuated in a dose dependent manner when treated with PPA (Fig. 2-9) corroborating that PPA induced a decrease in COX-2 which translated into a dramatic decrease in PGE₂. There was no significant difference in PGE₂ production between cells cultured in the presence of PPA and control cells (Fig. 2-10).

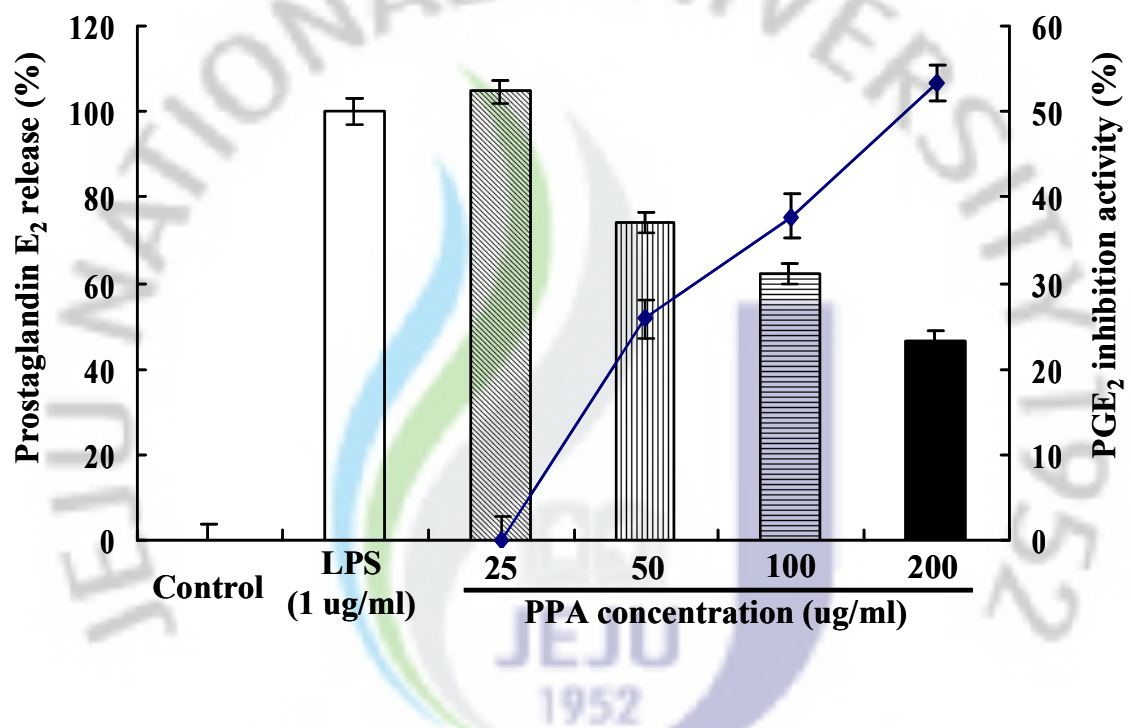


Fig. 2-10. Inhibition of isolated PPA on PGE₂ production in RAW 264.7 macrophage cells. PGE₂ production in supernatant fluid was measured using an ELISA kit. Experiments were performed in triplicate and the data are expressed as mean \pm SE.

4. DISCUSSION

Algal polysaccharides have been widely tested for their biological activities in vitro and in vivo. Because of their high biological activities, sulfated polysaccharides contained in algae are an alternative natural source for synthetic compounds in pharmaceutical industry.

In this study, the anti-inflammation activity of *E. cava* collected from Jeju Island was hydrolyzed by different enzymes and their anti-inflammatory activities were investigated. Several carbohydrases and proteases were used in this study to prepare enzymatic extracts and then were evaluated potential anti-inflammatory activities of *E. cava*. We showed the AMG digest has the highest inhibitory effects on NO production in LPS-stimulated RAW 264.7 cells. To identify the active compounds from the AMG digest, we performed the molecular membrane system, the ethanol separation, the anion exchange and gel permeation chromatography, and the 50 kDa over fraction, the crude polysaccharide (CPS) and the purified polysaccharide (PPA) were obtained. The PPA showed about 1381 kDa molecular weight and comprised mainly of fucose 82% and galactose 11%, (0.92 sulfated/total sugar).

The AMG digests' derivatives (50 kDa over fraction, CPS and PPA) significantly inhibited the NO production and PPA showed the highest inhibitory activity on NO production. Also, PPA decreased the prostaglandin-E₂ (PGE₂) production and suppressed the inducible nitric oxide synthase (iNOS) and cyclooxygenase-2 (COX-2) expression in the LPS-stimulated Raw 264.7 cells.

The present in vitro study shows that the release of pro-inflammatory mediators (PGE₂, NO) and the expression of COX-2 and iNOS genes were stimulated by incubation with

LPS (1ug/ml) for 24 hr in murine RAW 264.7 macrophages, and these effects could be modulated by PPA. The inhibitory effects on PGE₂ and NO production by PPA might be associated with their crucial effective treatment of animal respiratory tract diseases and mastitis. Both NO and prostaglandins (PGs) are well known to be important mediators of acute and chronic inflammation and are synthesized by nitric oxide synthase (NOS) and cyclooxygenase (COX) enzymes, respectively. There are three isoforms of NOS (constitutively expressed neuronal NOS (nNOS), endothelial NOS (eNOS) and iNOS) and two isoforms of COX (constitutively expressed COX-1 and the inducible isoform COX-2).

iNOS and COX-2 are up-regulated in response to inflammatory and pro-inflammatory mediators and their products can influence many aspects of the inflammatory cascade.

In this study, PPA inhibited the induction of iNOS protein expression as well as NO production in a dose-dependent manner in RAW 264.7 macrophages. Similarly, production of PGE₂ as well as COX-2 protein expression was also suppressed in a dose-dependently by PPA. Thus, the PPA inhibited NO and PGE₂ production through the inhibition of iNOS and COX-2 expression in LPS-stimulated RAW 264.7.

In summary, expression of iNOS and COX-2 genes were assessed as well as production of NO and PGE₂ by LPS-stimulated RAW 264.7 macrophages was evaluated. PPA was found to inhibit iNOS and COX-2 gene expression induced by LPS in dose-dependently as well as the subsequent production of NO and PGE₂ by LPS in RAW 264.7 macrophages. Therefore, we suggest that PPA might be effective as immunomodulatory mediator to elicit beneficial effects.

REFERENCE

- Aberhard E, Henderson SA, Arabolos NS, Griscavage JM, Castro FE, Barrett CT, Ignarro LJ. (1995). Nonsteroidal anti-inflammatory drugs inhibit expression of the inducible nitric oxide synthase gene. *Biochem. Biophys. Res. Commun.*, 208, 1053-1059.
- Adebajo MO, Gesser HD. (2001). ESR study of alkyl radicals absorbed on porous Vycor glass I. Build-up of methyl and ethyl radicals. *Appl Surf Sci* 171:120-124
- Ahn MJ, Yoon KD, Min S., Lee JS, Kim JH, Kim TG, Kim SH, Kim NG, Huh H, Kim J. (2004). Inhibition of HIV-1 reverse transcriptase and protease by phlorotannins from the brown alga *Ecklonia cava*. *Biol. Pharm. Bull.* 27, 544–547.
- AOAC. Official method of analysis of the association of official analytical chemists. (15th Ed). (1990). Washington D.C.
- Artan M, Li Y, Karadeniz F, Lee SH, Kim MM, Kim SK. (2008). Anti-HIV-1 activity of phloroglucinol derivative, 6,6'-bieckol, *Ecklonia cava*. *Bioorganic & Medicinal Chemistry*. 16, 7921-7926.
- Athukorala Y, Jung WK, Yasanthan T, Jeon YJ. (2006a). An anticoagulative polysaccharide from an enzymatic hydrolyaste of *Ecklonia cava*. *Carbohydr polymer*. 66:184-191.
- Boraschi D, Cifone M G, Falk W, Flad H D, Tagliabue A, Martin M U. (1998). Cytokines in inflammation. *Eur. Cytokine Netw.*, 9, 205-212.
- Cheng S C, Cheng S N, Andrew t, Chou T C. Anti-inflammatory activity of c-phycocyanin in lipopolysaccharide-stimulated RAW 264.7 macrophages. *Life Sciences*. 81, 1431-1435.

- Choi MS, Lee SH, Cho HS, Kim Y, Yun YP, Jung HY, Jung JK, Lee BC, Pyo HB, Hong JT, (2007). Inhibitory effect of obovatol on nitric oxide production and activation of NF-kappaB/MAP kinases in lipopolysaccharide-treated RAW 264.7 cells. *Eur. J. Pharmacol.* 556, 181–189.
- Conner EM, Grishman MB. (1996). Inflammation, free radicals, and antioxidants. *Nutrition*, 12(4), 274-277.
- Cortan RS, Kumar V, Robbins SL. (1994). pathologic basis of disease. 5, 51-92, Saunders.
- Dinarello C A. (2000). Pro-inflammatory cytokines. *Chest.*, 118, 503-508.
- Fubini B, Hubbard A. (2003): Reactive oxygen species (ROS) and reactive nitrogen species (RNS) generation by silica in inflammation and fibrosis. *Free Radical Biology and Medicine*, 34, 1507-1516.
- Fukuyama Y, Kodama M, Miura I, Kinzyo Z, Mori H, Nakayama Y, Takahashi M. (1990). Anti-plasmin inhibitor. VI. Structure of phlorofucofuroeckol A, a novel phlorotannin with both dibenzo-1,4-dioxin and dibenzofuran elements, from *Ecklonia kurome* Okamura. *Chem. Pharm. Bull.* 38, 133–135.
- Goldstein S, Meyerstein D, Czapski G. (1993). The Fenton reagents. *Free Radic. Biol. Med.*; 15: 435–445.
- Grisham M B. (1998). Reactive metabolites of oxygen and nitrogen, NF-kB and chronic inflammation. *Pathophysiology*, 5(1), 64.
- Han ES, Kim JW, Eom MO, Kang IH, Kang HJ, Choi JS, Ha KW, Oh HY. (2000). Inhibitory effect of *Ecklonia stolonifera* on gene mutation on mouse lymphoma tk^{+/+} locus in L5178Y-3.7.2.C cell and bone marrow micronuclei formation in ddY mice. *Environ. Mutagen Carcinogen* 20, 104–111.

- Harsharan S, Bhatia E C J, Antonio C P O., Olumayokun A, Olajide G M S, Bernd L F. (2008). Mangiferin inhibits cyclooxygenase-2 expression and prostaglandin E2 production in activated rat microglial cells. *Archives of Biochemistry and Biophysics*. 477:253-258.
- Hawkey C J. (1999). COX-2 inhibitors. *Lancet*, 353, 307-314.
- Henderson B, Poole S, Wilson M. (1996). Bacterial modulins: a novel class of virulence factors which cause host tissue pathology by inducing cytokine synthesis. *Microbiol. Rev.*, 60, 316-341.
- Heo SJ, Park EJ, Lee KW, Jeon YJ. (2005a). Antioxidant activities of enzymatic extracts from brown seaweeds. *Biores technol.* 96:1613-1623
- Heo SJ, Park PJ, Park EJ, Cho SK, Kim SK, Jeon YJ. (2005b). Antioxidative effect of proteolytic hydrolysates from *Eckonia cava* on radical scavenging using ESR and H₂O₂-induced DNA damage. *Food Sci Biotechnol.* 14:614-620
- Hla T, Neilson K. (1992). Human cyclooxygenase-2 cDNA. *Proc. Natl. Acad. Sci. U.S.A.*, 89, 7384-7388.
- J O'Neill L A, Kaltschmidt C. (1997). NF- κ B : a crucial transcription factor for glial and neuronal cell function. *Trends in Neurosciences*, 20(6), 252-258.
- Kabeya L M, Kanashiro A, Azzolini A E, Santos A C, Lucisano-Valim Y M. (2008). Antioxidant activity and cytotoxicity as mediators of the neutrophil chemiluminescence inhibition by butylated hydroxytoluene. *Pharmazie* 63, 67-70.
- Kang JS, Lee KH, Han MH, Lee HJ, Ahn JM, Han SB, Han GH, Lee KH, Park SK, Kim HM. (2008) *Phytotherapy Research*. 22, 883-888.
- Khodr B, Khalil Z. (2001). Modulation of inflammation by reactive oxygen species :

- implications for aging and tissue repair. *Free Radical Biology and Medicine*, 30(1), 1-8.
- Kim KN, Heo SJ, Song CB, Lee JH, Heo MS, Yeo IK, Kang KA, Hyun JW, Jeon YJ. (2006a). Protective effect of *Ecklonia cava* enzymatic extracts on hydrogen peroxide-induced cell damage. *Process biochem*. 41:2393-2401
- Kim KN, Lee KW, Song CB, Jeon YJ. (2006b). Cytotoxic activities of green and brown seaweeds collected from Jeju Island against four tumor cell lines. *J Food Sci Nutr*. 11:17-24
- Kooncumchoo P, Sharma S, Porter J, Govitrapong P, Ebadi M. (2006). Coenzyme Q10 provides neuroprotection in iron-induced apoptosis in dopaminergic neurons. *Journal of Molecular Neuroscience* 28, 125–142.
- Kubes P. (2000). Inducible nitric oxide synthase: a little bit of good in all of us. *Gut*, 47(1): 6-9.
- Lee DH, Kim NR, Lim BS, Lee YK, Yang HC. (2008). Effects of TGEDMA and HEMA on the expression of COX-2 and iNOS in cultured murine macrophage cells. *Dental material*.
- Lee JH, Kim ND, Choi JS, Kim YJ, Moon YH, Lim SY, Park KY. (1998). Inhibitory effects of the methanolic extract of an edible brown alga, *Ecklonia stolonifera* and its component, phloroglucinol on aflatoxin B1 mutagenicity in vitro (Ames test) and on benzo(a)pyrene or N-methyl N-nitrosourea clastogenicity in vivo (mouse micronucleus test). *Nat. Prod. Sci.* 4, 105–114.
- Liu ZQ, Stephen MW, Zhou HH. (1999). Specific of inducible nitric-oxide synthase inhibitors: prospects for clinical therapy. *Acta Pharmacol. Sin.*, 20(11): 1052-1056.
- MacMicking J, Xie Q W, Nathan C. (1997). Nitric oxide and macrophage function.

- Annu. Rev. Immunol.*, 15, 323-350.
- Matsuda H, Kageura T, Oda M, Morikawa T, Sakamoto Y, Yoshikawa M. (2001).
Effects of constituents from the bark of *Magnolia obovata* on nitric oxide production
in lipopolysaccharide-activated macrophages. *Chem. Pharm. Bull.* 49, 716–720.
- Miquel J, Quintanilha AT, Weber H. (1989). Handbook of free radicals and antioxidants
in biomedicine. Vol. 1, CRC Press, Boca Raton, Florida.
- Moncada S, Palmer RM, Higgs EA. (1992). Nitric oxide: physiology, pathophysiology.
Pharmacol. Rev., 43, 109-142.
- Nagayama K, Iwamura Y, Shibata T, Hirayama I, Nakamura T. (2002). Bactericidal
activity of phlorotannins from the brown alga *Ecklonia kurome*. *J. antimicrob.
Chemother.* 50, 889–893.
- Nathan C F. (1987). Secretory products of macrophages, *J. Clin. Invest.*, 79, 319-326.
- Needleman P, Isakson P C. (1998). Selective inhibition of cyclooxygenase 2. *Sci. Med.*,
1, 35-36.
- Nicod L P. (1993). Cytokines: overview. *Thorax*, 48, 660-667.
- Nordberg J, Arner E.S.J. (2001). Reactive oxygen species, antioxidants, and the
mammalian thioredoxin system. *Free Radical Bio Med* 31:1289-1312
- Nozik-Grayck E, Stenmark KR. (2007). Role of reactive oxygen species in chronic
hypoxia-induced pulmonary hypertension and vascular remodeling. *Advances in
Experimental Medicine and Biology* 618, 101–112.
- Oppenheim J J. (2001). Cytokines: past, present, and future. *Int. J. Hematol.*, 74, 38.
- O’Sullivan M G, Chilton F H, Huggins E M Jr., McCall C E. (1992).
Lipopolysaccharide priming of alveolar macrophages for enhanced synthesis of
prostanoids involves induction of a novel prostaglandin H synthase. *J. Biological.*

Chem., 267, 14547-14550.

- Park SY, Lee HJ, Yoon WJ, Kang GJ, Moon JY, Lee NH, Kim SJ, Kang HK, Yoo ES. (2005). Inhibitory effects of Eutigosides isolated from *Eurya emarginata* on the inflammatory Mediators in RAW 264.7 cells. *Arch Pharm Res.* 28(11), 1244-1250
- Rajapakes N, Kim MM, Mendis E, Kim SK. (2007). Inhibition of inducible nitric oxide synthase and cyclooxygenase-2 in lipoolysaccharide-stimulated RAW264.7 cells by carboxybutyrylated glucosimine takes place via down-regulation of mitogen-activated protein kinase-mediated factor- κ B signaling.. *Immunology.*123, 348-357.
- Rouveix B. (1997). Clinical pharmacology of cytokines. *Eur. Cytokine Netw.*, 8, 291-293.
- Shin EM, Zhou HY, Guo LY, Kim JA, Lee SH, Merfort I, Kang SS, Kim HS, Kim SH, Kim YS. (2008). Anti-inflammatory effects of glycyrol isolated from *glycyrrhiza uralensis* in LPS-stimulated RAW 264.7 macrophages. *International Immunopharmacology.* 8, 1524-1532
- Sies H. (1985). Oxidative stress: oxidants and antioxidants. Academic Press, New York.
- Singh S, Evans TW. (1997). Nitric oxide, the biological mediator of the decade: fact or fiction. *Eur. Respir. J.*, 10. 699-707.
- Son HJ, Lee HJ, Choi YHS, Ryu JH. (2000). Inhibitors of nitric oxide synthesis and TNF-alpha expression from *Magnolia obovata* in activated macrophages. *Planta Med.* 66, 469-471.
- Speakman JR. (2003). Oxidative phosphorylation, mitochondrial proton cycling, free radical production and aging. *Advances in Cell Aging and gerontology*, 14, 35-68.)
- Suzuki Eriko, Sugiyama Chie, Umezawa Kazuo. (2008). Inhibition of inflammatory mediator secretion by (-)-DHMEQ in mouse bone marrow-derived macrophages.

- Biomedicine & Pharmacotherapy*. 1-8.
- Tao JY, Zhao L, Huang Zj, Zhang XY, Zhang SL, Zhang QG, Fei-Xiao, Zhang BH, Feng QL, Zheng GH. (2008). *Inflammation*. 3, 31.
- Trowbridge HO, Emiling R C. (1997). In inflammation: a review of the process. 5 th Ed. Quintessence Pub. Co., Chicago.
- Turcanu V, Williams N A. (2001). Cell identification and isolation on the basis of cytokine secretion: a novel tool for investigating immune responses. *Nat. Med.*, 7, 373-376.
- Ulevitch R J, Tobias P S. (1995). Receptor-dependent mechanisms of cell stimulation by bacterial endotoxin. *Annu. Rev. Immunol.*, 13, 437-457.
- Valentin AP, Hong W, Christopher JC, Steven GF, Keven JT. (2003). The Cholinergic Anti-inflammatory pathway: A missing link in neuroimmuno-modulation. *Molecular medicine*, 9, 125-134.
- Vane J. R, Bakhle Y S, Botting R M. (1998). Cyclooxygenases 1 and 2. *Annual Rev. Pharmacol. Toxicol.*, 38, 97-120.
- Walling C. (1975). Fenton's reagents revisited. *Acc. Chem. Res.* 8: 125-131.
- Yu GL, Hung TM, Bae KH, Shin EM, YuZhou H, Hong YN, Kang SS, Kim HP, Kim WS. (2008). *European journal of pharmacology*. 591, 293-299.
- Zhou HY, Shin EM, Go LY, Youn UJ, Bac KH, Kang SS, Zou Lb, Kim YS. (2008). Anti-inflammatory activity of 4-methoxyhonokiol is a function of the inhibition of iNOS and COX-2 expression in RAW 264.7 macrophages via NK-kB, JNK and p38 MARK inactivation. *European Journal of Parmacology*. 586, 340-349.

ACKNOWLEDGEMENT

철 없던 학부 3학년부터 고된 석사 2년 과정까지 4년이라는 시간 동안 실험실에서 연구 생활을 하였습니다. 연구 생활 동안에 힘들고 기쁠 때 언제나 함께해주시고, 못한 제자를 옹운 길로 인도해주신 전유진 교수님께 고개 숙여 감사의 마음을 전합니다. 또한, 부모님같이 신경을 써주시고 사랑을 베풀어 주신 이기완 교수님과 바쁘신 와중에도 논문의 심사와 많은 조언을 해주신 허문수 교수님께 감사를 드립니다. 학부 시절과 석사 과정 동안 가르쳐주시고 보살펴 주신 송춘복 교수님, 이제희 교수님, 여인규 교수님, 이영돈 교수님, 최광식 교수님, 이경준 교수님, 김기영 교수님, 정준범 교수님께 감사를 드립니다. 그리고 항상 아껴주시고 신경을 써주신 식품공학과 김수현 교수님과 하진환 교수님께 감사를 드립니다.

4년이라는 시간 동안의 제 삶과 함께 했던 해양생물자원이용공학연구실, 그 속에 하늘 같은 김원석 선배님, 양현필 선배님과 연구와 삶의 스승으로 생각하는 허수진 선배님, 오영빈 선배님, 김길남 선배님, 이승홍 선배님, 외국인이지만 한국인보다 더 선한 마음을 가진 Yasantha, Mahinda, 누나 같이 신경 써주었고 연구 선배이자 동기인 차선희, 안긴내, 같이 졸업하며 언제나 멋진 실장 석천이, 친남동생 같은 원우, 우석이, 민철이, 인환이, 친여동생 같은 주영이, 혜미, 석경이, 언제나 당차며 졸업하는데 도움을 준 희정이, 졸업 관련 실험에 큰 도움이 되어주시고 많은 사랑과 조언을 베풀어주신 정원교 선배님과 이상훈 선배님, 다른 실험실에 있어도 가족같이 아껴주신 치훈이형, 맹진이형, 문휴형, 영건이형, 철홍이형, 상규형, 경주형, 송헌이형, 주상이형, 태원이형, 민주, 혜영이, 미란이, 기천이에게 감사의 마음을 전하며, 우리 실험실 후배 같은 익수, 용재, 창영, 영화, 유철, 고마운 마음을 전합니다. 아울러, 같이 졸업하고 서로 힘이 되어주는 믿음직한 동기인 영득, 윤범, 민석, 봉근이, 상혁이, 봉규 그리고 이 자리에 함께 하지는 못하지만 하늘에서 지켜봐준 현석이에게도 고마운 마음을 전합니다. 그리고 뒤에서 격려와 응원 해주신 아쿠아그

런택(ㄸ)의 제종선 전무님과 이정석 박사님께도 감사를 드립니다.

그리고 28년이라는 시간 동안 사랑과 정성을 쏟아주시며 묵묵히 바라봐 준 아버지, 어머니, 항상 동생 잘 되기만을 바라는 큰 누님, 작은 누님, 형님, 그리고 나를 믿고 도와 주신 친척 가족들에게도 감사의 마음을 전합니다.

저희 주위에 있거나 혹은 다른 곳에서 저를 도와주시고 생각해 주시는 모든 분들께 고마운 마음을 전합니다.

마지막으로 항상 저와 함께 실험실 생활을 하면서 힘들고 슬플 때, 즐겁고 기쁠 때 언제나 함께 해준 실험실 후배이자 사랑하는 김아름다슬, 그리고 뒤에서 격려와 응원해 주신 아람이의 부모님께 감사의 마음을 전합니다.

